REPORT DOCUMENTATION PAGE

Form Approved
OMB No 0704-0188

REPORT DATE	3. REPORT TYPE AND DATES COVERED
April 22, 1994	TECHNICAL REPORT

4. TITLE AND SUBTITLE

A Combined Experimental and Theoretical Study of the Neutral, Cationic and Anionic Si_3N Cluster Molecule

5. FUNDING NUMBERS

G N00014-89-J-1497
R&T 4131050

6. AUTHOR(S)

N. Gorldberg, M. Iraqi, H. Schwarz, A. I. Boldyrev and Jack Simons

7. PERFORMING ORGANIZATION NAME(S) AND ADDRESS(ES)

UNIVERSITY OF UTAH
DEPARTMENT OF CHEMISTRY
SALT LAKE CITY, UTAH 84112
U.S.A.

8. PERFORMING ORGANIZATION REPORT NUMBER

Technical Report No. 46

9. SPONSORING / MONITORING AGENCY NAME(S) AND ADDRESS(ES)

OFFICE OF NAVAL RESEARCH
CHEMISTRY PROGRAM
800 NORTH QUINCY ST.
ARLINGTON, VIRGINIA 22217-5000

10. SPONSORING / MONITORING AGENCY REPORT NUMBER

11. SUPPLEMENTARY NOTES

Submitted for publication in the Journal of Chemical Physics

12a. DISTRIBUTION / AVAILABILITY STATEMENT

THIS DOCUMENT HAS BEEN APPROVED FOR PUBLIC RELEASE AND SALE; ITS DISTRIBUTION IS UNLIMITED

12b. DISTRIBUTION CODE

UNLIMITED

13. ABSTRACT *(Maximum 200 words)*

Collision experiments and high-level ab initio calculations are used for the first characterization of the neutral, cationic and anionic Si_3N cluster molecules. The experimentally observed fragmentation processes are well described by calculated reaction energies of all dissociation channels. In addition, the geometries and harmonic frequencies of Si_nN (n=1-3) have been calculated for the cationic, anionic and neutral species.

14. SUBJECT TERMS

15. NUMBER OF PAGES

16. PRICE CODE

17. SECURITY CLASSIFICATION OF REPORT	18. SECURITY CLASSIFICATION OF THIS PAGE	19. SECURITY CLASSIFICATION OF ABSTRACT	20. LIMITATION OF ABSTRACT
UNCLASSIFIED	UNCLASSIFIED	UNCLASSIFIED	

OFFICE OF NAVAL RESEARCH

Contract N00014-89-J-1497

R&T Code 4131050
Scientific Officer: Dr. R. Nowak

Technical Report No. 46

A Combined Experimental and Theoretical Study of the Neutral, Cationic and Anionic Si_3N Cluster Molecule"

by

N. Goldberg, M. Iraqi, H. Schwarz, A. I. Boldyrev, and J. Simons

Prepared for Publication in

The Journal of Chemical Physics

The University of Utah
Department of Chemistry
Salt Lake City, Utah 84112-1194

April 22, 1994

A Combined Experimental and Theoretical Study of the Neutral, Cationic and Anionic Si_3N Cluster Molecule

Norman Goldberg, Muhammad Iraqi and Helmut Schwarz*

Institut fur Organische Chemie der Technischen Universitat Berlin, Strasse des 17 Juni, D-10623 Berlin, Germany.

Alexander Boldyrev and Jack Simons*

Department of Chemistry, The University of Utah, Salt Lake City, Utah 84112, USA.

ABSTRACT

Collision experiments and high-level ab initio calculations are used for the first characterization of the neutral, cationic and anionic Si_3N cluster molecules. The experimentally observed fragmentation processes are well described by calculated reaction energies of all dissociation channels. In addition, the geometries and harmonic frequencies of Si_nN (n=1-3) have been calculated for the cationic, anionic and neutral species.

I. INTRODUCTION

In the last couple of years the search for new materials that possess unique physical properties has been going through a revival phase. Especially the development of novel sophisticated experimental techniques, such as laser desorption (LD) and chemical-vapor deposition (CVD) have led to the generation of hitherto unknown, unusual compounds. Amongst these materials, carbon- and silicon-containing nitrides have received special interest.[1] Thus, the covalently bound polymer carbon(IV) nitride has only recently been synthesized by a combination of LD and CVD techniques.[2] This structurally not yet fully characterized substance seems to exhibit the theoretically predicted physical properties such as an extreme hardness and diatomic-like modules of elasticity. It is believed to possess a structure similar to the binary silicon nitride β-Si_3N_4.

In general, it is known that the p-block main-group elements form nitrides with exceptional chemical inertness and mechanical hardness.[3] However, binary silicon nitrides are not only of interest to material scientists. Small silicon-containing clusters are believed to be formed in silicon-etching processes and thus, as they can also be viewed upon as prototypes for the interaction of main-group elements with silicon sites in clusters and surfaces, have received much attention by experimentalists[4] as well as theoreticians.[5]

To our knowledge there exists only very little information on small binary silicon-nitrogen clusters. Recently, Brodie et al.[4d] have carried out pyrolysis-solid-state NMR studies on silazanes in order to obtain mechanistic insight into the genesis of the siliconnitride solid (β-Si_3N_4), and some of us have been able to characterize the Si_2N and Si_2O cluster molecules[4e] by neutralization-reionization mass spectrometry (NRMS).[6] This mass spectrometric technique

has been applied successfully for the generation of numerous elusive silicon-containing molecules, which due to the facile intermolecular reactions could not be studied in the condensed phase.[7]

In this publication we wish to report the results of combined experimental and ab initio investigations on the hitherto unknown Si_3N cluster and its cationic Si_3N^+ and anionic Si_3N^- counterparts. The cationic and neutral species have been structurally characterized by collisional-activation and neutralization-reionization mass spectrometry.[8] High-level ab initio methods have been employed for the structural and energetic description of the various experimentally observed neutral, cationic and anionic Si_nN and Si_n (n=1-3) molecules. Calculated structural data of the experimentally observed species will be given together with vibrational spectra to facilitate the spectroscopic observation of these novel molecules.

II. EXPERIMENTAL DETAILS

The collision experiments were performed in a substantially modified ZAB four sector tandem mass spectrometer with BEBE modification (B stands for magnetic and E for electrostatic analyzer). For a detailed description of the mass spectrometer the reader is refereed to previous publications.[9] For the cluster generation, trisilylamine, $N(SiH_3)_3$ was used as the precursor molecule. This compound was prepared via standard literature procedures.[10] Care had to be taken to avoid possible leaks in the inlet system because oxygen traces can lead to sudden explosion of the amine. The sample was introduced into the ion source of the mass spectrometer through a chemical ionization gas inlet system. The cationic cluster could easily be obtained upon dissociative electron impact ionization of $N(SiH_3)_3$. The source conditions were as follows: electron energy

50 eV; repeller voltage ca. 30 V; ion source temperature, 200°C; accelerating voltage 8 kV. The ions of interest were mass selected by means of (B1)(E1). Collision experiments were performed with 80% transmittance (T) of the ion beam in order to ensure single-collision conditions. In the case of the collisional activation (CA) mass spectrum, helium was introduced as a collision gas into the second part of a differentially pumped tandem collision cell. For the neutralization-reionization experiments xenon was used as the neutralization agent in the first part of the tandem collision cell. The remaining ions were electrostatically deflected from the beam by means of an electrode (charged to 1000 V) situated between the two collision cells. The neutral molecules were reionized by colliding the beam with oxygen, For a particle m/z=98 having been accelerated to 8 keV-energy it takes approximately 6 microseconds to travel from the first to the second collision cell, thus providing a lower limit for the minimal lifetime of the neutral molecule. The ionic dissociation products were recorded by scanning the second magnetic analyzer (B2). To improve the signal-to-noise-ratio of the spectra the data of 20-50 accumulated scans were on-line processed with an AMD-Intectra data system.

II. COMPUTATIONAL DETAILS

The bond lengths and angles of neutral, cationic and anionic SiN, Si_2N, and Si_3N, as well as Si_2 and Si_3 were optimized by employing analytical gradients[11] using the Gaussian 92 program[12] with polarized split-valence basis sets (6-311+G*)[13,14] at the SCF and the MP2(full) level (USCF and UMP2(full) for open shell systems of theory). Our optimal-geometric parameters are presented in Fig. 1 and our simulated IR-spectra based on the MP2(full)/6-311+G* calculated frequencies and their intensities are drawn in Fig. 2.

The MP2(full)/6-311+G* equilibrium geometries were used to evaluate electron correlation corrections in the frozen-core approximation by full fourth order[15] Møller-Plesset perturbation theory and by the (U)QCISD(T) method[16] using 6-311+G(2df) basis sets. The USCF wave functions for open shell systems were projected to pure spectroscopic states for which the corresponding results are denoted PUSCF, PMP2, PMP3 and PMP4.[17] Calculated reaction energies and available experimental data are presented in Table I.

IV. THEORETICAL RESULTS

SiN, SiN^+ and SiN^-. The neutral SiN molecule is known to have a doublet $^2\Sigma^+$ ($1\sigma^2 2\sigma^2 1\pi^4 3\sigma^1$) ground electronic state.[18,19] The lowest excited state $^2\Pi_i$ ($1\sigma^2 2\sigma^2 1\pi^3 3\sigma^2$) is only 0.25 eV higher in energy.[19] At our highest level (QCISD(T)+ZPE), the $^2\Sigma^+$ state is indeed found to be the ground state and the first excited $^2\Pi_i$ state is 0.35 eV higher in energy. Our calculated bond length R_e(Si-N)=1.53 Å for the ground $^2\Sigma^+$ state at the MP2(full)/6-311+G* level is somewhat shorter than the experimental value 1.57 Å.[18,19] To the best of our knowledge, experimental structural data on SiN^+ and SiN^- are not known.

From the $^2\Sigma^+$ and $^2\Pi_i$ electronic states of the SiN molecule, the two cationic triplet $^3\Sigma^-$ ($1\sigma^2 2\sigma^2 1\pi^2 3\sigma^2$) and $^3\Pi$ ($1\sigma^2 2\sigma^2 1\pi^3 3\sigma^1$) states are expected to be the most stable. Bruna, Peyerimhoff and Buenker (BPB)[20] studied five low-lying $^3\Sigma^-$ ($1\sigma^2 2\sigma^2 1\pi^2 3\sigma^2$), $^3\Pi$ ($1\sigma^2 2\sigma^2 1\pi^3 3\sigma^1$), $^1\Pi$ ($1\sigma^2 2\sigma^2 1\pi^2 3\sigma^2$), $^1\Sigma^+$ ($1\sigma^2 2\sigma^2 1\pi^4$) and $^1\Delta$ ($1\sigma^2 2\sigma^2 1\pi^2 3\sigma^2$) electronic states of SiN^+ using large-scale CI calculations and found that the $^3\Sigma^-$ is the most stable and the first $^3\Pi$ state is 0.21 eV higher in energy.[20] We repeated the calculations of the both the $^3\Sigma^-$ and $^3\Pi$ states at the MP2(full)/6-311+G* level and our bond lengths R_e(Si-

N)=1.78 Å ($^3\Sigma^-$) and R_e(Si-N)=1.65 Å ($^3\Pi$) reasonably agree with the R_e(Si-N)=1.81 Å ($^3\Sigma^-$) and R_e(Si-N)=1.71 Å ($^3\Pi$) BPB data.[13] Our ($^3\Sigma^+ \rightarrow {}^3\Pi$) excitation energy (0.13 eV) is also close to the 0.21 eV BPB value. Our first adiabatic IE for SiN is 10.0 eV at the QCISD(T) level.

The experimental electron affinity is not known for SiN. The lowest singlet anion electronic state $^1\Sigma^+$ ($1\sigma^2 2\sigma^2 1\pi^4 3\sigma^2$) may be derived from either the ground or the first excited electronic state of neutral SiN when an electron is added to the lowest energy available MO. The isoelectronic SiO molecule has a singlet $^1\Sigma^+$ ($1\sigma^2 2\sigma^2 1\pi^4 3\sigma^2$) ground state with its first excited state lying more than 4 eV higher in energy.[18] Therefore we studied only the $^1\Sigma^+$ state for SiN^-.

The optimized bond lengths and vibrational frequencies at the MP2(full)/6-311+G* level are: 1.63 Å and 1005 cm^{-1}, which agree well with results of Peterson and Woods[21] R_e(Si-N)=1.605 Å and ω_e=1092 cm^{-1} for SiN^- ($^1\Sigma^+$) at the MP4 level. The first adiabatic electron affinity of SiN is found to be 3.36 eV at the PMP4 level and 2.91 eV at the QCISD(T) level, both of which are lower than the experimental EA (3.821 eV)[22] of the valence isoelectronic CN molecule. The electron affinity of SiN calculated indirectly by Peterson and Woods is 3.32 eV.[21] Dissociation energies (at the QCISD(T)level) for SiN^+ into Si^+ + N, SiN into Si + N and SiN^- into Si^- + N are: 52 kcal/mol, 96 kcal/mol and 135 kcal/mol, respectively.

Si_2N, Si_2N^+ and Si_2N^-. The neutral Si_2N molecule and Si_2N^+ cation were recently observed in mass spectrometric studies,[4e] but to our knowledge, there exist no analogous experimental data on Si_2N^-, and theoretical data are not available for any of these species.

We optimized the geometry for the cation Si_2N^+ using the MP2(full)/6-311+G* method starting from an angular C_{2v} ($^1A_1$) structure with an initial SiNSi

angle equal to 140°. We converged to R_e(Si-N)=1.631 Å, and a valence angle of Si-N-Si=180°. That is, the optimal structure I (geometry shown in Fig. 1 and simulated IR-spectrum in Fig. 2) of $SiNSi^+$ is linear $D_{\infty h}$ ($^1\Sigma_g^+$: $1\sigma_g^2 1\sigma_u^2 2\sigma_g^2 1\pi_u^4 2\sigma_u^2 1\pi_g^0$), which is different from the isoelectronic SiCSi molecule,[23,24] which has a singlet bent C_{2v} ($^1A_1$) structure. Our most favorable dissociation energies (at the QCISD(T) level, see Table 1) for Si_2N^+ is into Si^+ + SiN (+167 kcal/mol).

We optimized the geometry for both linear $D_{\infty h}$ ($^2\Pi_g$: $1\sigma_g^2 1\sigma_u^2 2\sigma_g^2 1\pi_u^4 2\sigma_u^2 1\pi_g^1$) and bent C_{2v} ($^2A_1$: $1a_1^2 1b_2^2 2a_1^2 1b_1^2 3a_1^2 2b_1^2 4a_1^1$) structures of Si_2N. At the MP2(full)/6-311+G* level, the C_{2v} is a minimum (see the structure II in Fig. 1 and the simulated IR-spectrum in Fig. 2), but the $D_{\infty h}$ ($^2\Pi_g$) structure III has one imaginary frequency whose eigenvector leads to a linear $C_{\infty v}$ ($^2\Pi$: $1\sigma^2 2\sigma^2 3\sigma^2 1\pi^4 4\sigma^2 2\pi^1$) structure IV which is only 0.36 kcal/mol lower in energy at this level of theory. Optimization of the $C_{\infty v}$ ($^2\Pi$) structure within the MP2(full)/6-311+G* framework gives a minimum with <u>two nonequivalent bond lengths</u> $R_e(Si_1\text{-}N)$=1.573 Å and $R_e(Si_2\text{-}N)$=1.694 Å. The distortion of S_2N from $D_{\infty h}$ into $C_{\infty v}$ symmetry at MP2(full) level is due to an artifactual symmetry breaking. For our large 6-311+G(2df) basis sets, the energy of the linear $D_{\infty h}$ structure III is lower at <u>all</u> correlated levels (from PMP2 to QCISD(T)) than the $C_{\infty v}$ structure IV using MP2(full)/6-311+G* geometries for both structures. Therefore we optimized the geometry of linear SiNSi at the QCISD(T)/6-311+G* level, where we found no symmetry breaking problem. The linear $D_{\infty h}$ ($^2\Pi_g$) structure is a minimum with R_e(Si-N)=1.643 Å and $\nu_1(\sigma_g)$=613 cm^{-1}, $\nu_2(\pi_u)$=221 cm^{-1}, $\nu_2'(\pi_u)$=130 cm^{-1} and $\nu_3(\sigma_u)$=898 cm^{-1} (simulated IR-spectrum is shown in Fig. 2). Therefore the global minimum of the Si_2N molecule has a linear $D_{\infty h}$ ($^2\Pi_g$) structure.

Both II and III structures of Si_2N are very close in energy and may coexist in the gas phase. According to our calculations, the energetically favored dissociation path for Si_2N is into SiN + Si (+125 kcal/mol); dissociation into Si_2 + N (+152 kcal/mol) is less favorable. Finally, the adiabatic ionization energy of Si_2N is predicted to be 6.2 eV (see Table 1).

The Si_2N^- anion is isoelectronic with the neutral Si_2O molecule and, according to previous calculations,[5b] the angular C_{2v} ($^1A_1$) structure of Si_2O is the most stable, but two linear SiOSi ($D_{\infty h}$,$^3\Sigma_g^-$) and SiSiO ($C_{\infty v}$,$^3\Sigma^-$) structures are 18-27 kcal/mol higher in energy. We optimized the geometry for all of these three structures of Si_2N^-: V (C_{2v} , $^1A_1$: $1a_1^2 1b_2^2 2a_1^2 1b_1^2 3a_1^2 2b_1^2 4a_1^2$), VI ($D_{\infty h}$, $^3\Sigma_g^-$: $1\sigma_g^2 1\sigma_u^2 2\sigma_g^2 1\pi_u^4 2\sigma_u^2 1\pi_g^2$) and VII ($C_{\infty v}$, $^3\Sigma^-$: $1\sigma^2 2\sigma^2 3\sigma^2 1\pi^4 4\sigma^2 2\pi^2$), and found that all three structures are local minima with the singlet V structure being the most stable, as in the case of Si_2O.[5b] However, the linear VI structure is only 5.0 kcal/mol higher in energy at the PMP4/6-311+G(2df) level and 1.7 kcal/mol at the QCISD(T)/6-311+G(2df) level. The VII structure is 39.6 kcal/mol (at the QCISD(T)/6-311+G(2df) level) higher in energy than the most stable V. The geometries of all these structures are presented in Fig. 1 and the simulated IR-spectra are shown in Fig. 2.

These energy data indicate that the Si_2N^- anion may coexist in two molecular forms in the gas phase. Electron photodetachment experiments of Si_2N^- may allow experimental verification of these predictions. Our calculated adiabatic electron affinity is $EA_a(Si_2N)$=1.1 eV for Si_2N. Our most favorable dissociation energies (at the QCISD(T) level, see Table 1) for Si_2N^+ into Si^+ + SiN, Si_2N into Si + SiN and Si_2N^- into SiN^- + Si are: 167 kcal/mol, 125 kcal/mol and 80 kcal/mol, respectively.

Si_3N, Si_3N^+ and Si_3N^-. We initially performed calculations on Si_3N^+ at the SCF/6-311+G* level and found the high symmetry D_{3h} structure (with $1a_1'^2 1e'^4 2a_1'^2 1a_2''^2 2e'^4 3e'^2$ electronic configuration) to not be a local minimum either in its triplet, or singlet states. The triplet D_{3h} ($^3A'$) structure VIII (Fig. 1) has two imaginary frequencies with two eigenvectors leading to the Y-type structure IX and to the T-type structure X (both have the same electronic configuration: C_{2v}, $^3B_2$, $(1a_1^2 1b_2^2 2a_1^2 3a_1^2 1b_1^2 4a_1^2 2b_2^2\ 3b_2^1 5a_1^1)$. The structures IX and X (Fig. 1) are local minimum and saddle point, respectively. The barrier for intramolecular preudorotation (top of the barrier corresponding to the structure X) is 3.4 kcal/mol at the SCF/6-311+G*+ZPE level. The other triplet (C_{2v}, $^3B_1$, $1a_1^2 1b_2^2 2a_1^2 3a_1^2 1b_1^2 4a_1^2 2b_2^2\ 2b_1^1 5a_1^1$) state is a local minimum at the Y-type structure XI. This structure, relative to the IX structure, is 2.4 kcal/mol (at SCF/6-311+G*) higher in energy. However both of the triplet minima are higher in energy than the singlet surface of the Si_3N^+ cation.

The high symmetry singlet D_{3h} ($^1A_1$ with $1a_1'^2 1e'^4 2a_1'^2 1a_2''^2 2e'^4 3e'^2$ electronic configuration) structure is not expected to be a minimum because of Jahn-Teller distortion which leads to the Y-type (XII) and the T-type (XIII) of structures. The singlet XII structure (C_{2v}, $1a_1^2 2a_1^2 1b_2^2 3a_1^2 1b_1^2 4a_1^2 2b_2^2\ 5a_1^2$) is found to be a saddle point, whereas the singlet XIII structure (C_{2v}, $1a_1^2 1b_2^2 2a_1^2 1b_1^2 3a_1^2 2b_2^2 4a_1^2 3b_2^2$) is a global minimum for Si_3N^+ at the SCF/6-311+G* level. The barrier for intramolecular pseudorotation is 7.0 kcal/mol (SCF/6-311+G*+ZPE). At the SCF level, the singlet potential energy surface is lower in energy than the lowest triplet $^3B_2$ potential energy surface by more than 10 kcal/mol. Because the singlet surface is expected to be even more stable at correlated levels, we studied only the singlet structures XII and XIII at the MP2(full)/6-311+G* level.

We optimized the geometry and calculated the harmonic frequencies for the singlet XII and XIII structures at the MP2(full)/6-311+G* level. These structures are shown in Fig. 1 and the vibrational spectrum of XIII is shown in Fig. 2. At MP2(full)/6-311+G* level, XIII is a global minimum (similar to the isoelectronic Si_3C molecule[25,26]) and XII is a saddle point. However at this level the pseudorotation barrier is substantial (17.3 kcal/mol including ZPE correction). The global minimum structure XIII was calculated at the QCISD(T) and PMP4 levels to obtain a more accurate dissociation energy. According to our calculations, among all possible dissociational channels Si_3N^+ into Si + Si_2N^+ (66 kcal/mol at QCISD(T) see Table 1) has the lowest energy.

From the order of the orbitals in Si_3N^+ (D_{3h}), we predict that the neutral Si_3N molecule has occupation $1a_1'^2 1e'^4 2a_1'^2 1a_2''^2 2e'^4 3e'^3$ in the high symmetry D_{3h} ($^2E'$) structure, which is not expected to be a minimum because of the Jahn-Teller distortion, which leads to the Y-type ($^2B_2$, $1a_1^2 2a_1^2 1b_2^2 3a_1^2 1b_1^2 4a_1^2 2b_2^2 5a_1^2\ 3b_2^1 2b_1^0 1a_2^0$) and T-type ($^2A_1$, $1a_1^2 2a_1^2 1b_2^2 3a_1^2 1b_1^2 4a_1^2 2b_2^2 5a_1^1 3b_2^2\ 2b_1^0 1a_2^0$) structures. Because orbitals other than the $5a_1$ and $3b_2$ low-lying orbital may play important roles, we further studied all configurations obtained by distributing three electrons among the $5a_1$, $3b_2$, $2b_1$, and $1a_2$ low-lying orbitals with doublet or quartet coupling of spins.

The doublet coupling leads to twelve states: C_{2v} symmetry $^2A_1$ ($5a_1^1 3b_2^2 2b_1^0 1a_2^0$, structure XIV), $^2A_1$ ($5a_1^1 3b_2^0 2b_1^2 1a_2^0$, structure XV), $^2A_1$ ($5a_1^1 3b_2^0 2b_1^0 1a_2^2$, structure XVI), $^2B_2$ ($5a_1^2 3b_2^1 2b_1^0 1a_2^0$, structure XVII), $^2B_2$ ($5a_1^0 3b_2^1 2b_1^2 1a_2^0$, structure XVIII), $^2B_2$ ($5a_1^0 3b_2^1 2b_1^0 1a_2^2$, structure XIX), $^2B_1$ ($5a_1^2 3b_2^0 2b_1^1 1a_2^0$, structure XX), $^2B_1$ ($5a_1^0 3b_2^2 2b_1^1 1a_2^0$, structure XXI), $^2B_1$ ($5a_1^0 3b_2^0 2b_1^1 1a_2^2$, structure XXII), $^2A_2$ ($5a_1^2 3b_2^0 2b_1^0 1a_2^1$, structure XXIII), $^2A_2$ ($5a_1^0 3b_2^2 2b_1^0 1a_2^1$, structure XXIV), $^2A_2$ ($5a_1^0 3b_2^0 2b_1^2 1a_2^1$,

structure XXV). Quartet coupling of the spins leads to four states: $^4A_2$ ($5a_1^1 3b_2^1 2b_1^1 1a_2^0$, structure XXVI), $^4B_1$ ($5a_1^1 3b_2^1 2b_1^0 1a_2^1$, structure XXVII), $^4B_2$ ($5a_1^1 3b_2^0 2b_1^1 1a_2^1$, structure XXVIII), $^4A_1$ ($5a_1^0 3b_2^1 2b_1^1 1a_2^1$, structure XXIX). The optimal geometries and relative energies of all of these structures at the SCF/6-311+G* level are presented in Fig. 1. According to the SCF/6-311+G* calculations, XXI is the global minimum but a few other structures lie within a few kcal/mol.

At SCF/6-311+G* level, XV, XVI, XVII, XX, XXI, XXII, XXV, XXVI, XXVII and XXVIII are local minima, XIV, XIX, XXIII, XXIV, XXIX are first order saddle points, and XVIII is second order saddle point. Our search for the global minimum was subsequently expanded to C_s symmetry structures and four additional doublet (^{2}A' and ^{2}A") and quartet (^{4}A' and ^{4}A") structures were studied at the SCF/6-311+G* level. The ^{2}A" state collapsed to XX or XXI depending on the starting geometry. The ^{2}A' state has a local minimum with the structure XXX (Fig. 1), but this lies 19.3 kcal/mol higher in the energy than global minimum at this level. The ^{4}A" state converges to the lowest quartet structure XXVI and ^{4}A' state has a local minimum with the structure XXXI (Fig. 1)18.2 kcal/mol higher in energy than global minimum.

Several of the lowest energy structures (XIV, XVII, XX, XXI, XXIV, XXVIII and XXIX) identified as detailed above, have been optimized at the MP2(full)/6-311+G* level (Fig. 1) and the relative energies of the rest of the structures have been calculated at MP2(full)/6-311+G* level using UHF/6-311+G* geometry. According to our calculations, XXI and XXIV has the lowest energies at MP2 level. The XXIV (C_{2v}, $^2A_2$) structure is predicted to be the lowest, with the XXI (C_{2v}, $^2B_1$) only 0.05 kcal/mol (MP2(full)/6-311+G*) higher in energy. However, only the XXI structure is a true minimum (its geometry is shown in Fig. 1 and its simulated IR-spectrum is presented in Fig. 2) while the XXIV structure is a

saddle point, whose eigenvector of imaginary frequency produces an in-plane distortion. Further geometry optimization of this Si_3N structure within C_s symmetry was not successful due to poor SCF convergence. However we do not expect structures with C_s symmetry will differ much in energy from the energy of XXIV.

Both neutral Si_2N and Si_3N species have two isomers that differ by only a few kcal/mol which is different from Si_2C, Si_3C and Si_2O, Si_3O, where the ground state structure is well separated in energy from other structures.

Our computed adiabatic ionization energy of Si_3N is 6.3 eV and the most energetically favored dissociation energy is 73 kcal/mol into Si_2N + Si, which is much lower than the dissociation energy of Si_2N into SiN + Si (see Table I). All these number should be considered as a preliminary estimate.

Based on the energy ordering of the neutral Si_3N molecule at MP2(full)/6-311+G* level (Fig. 1), we studied two low-lying anionic states of Si_3N^-: structure XXXIII (C_{2v}, $^1A_1$:$1a_1^2 1b_2^2 2a_1^2 3a_1^2 1b_1^2 2b_2^2 4a_1^2\ 3b_2^2 1a_2^2$) and structure XXXIII ($C_{2v}$, $^1A_1$:$1a_1^2 1b_2^2 2a_1^2 3a_1^2\ 1b_1^2 2b_2^2 4a_1^2 3b_2^2 2b_1^2$) (geometries are presented in Fig. 1). However both of these structures are found to not correspond to local minima. The XXXII structure has two imaginary frequencies and XXXIII has one imaginary frequency. The latter structure is lower in energy and its eigenvector of imaginary frequency produces an in-plane distortion. Geometry optimization of the Si_3N^- starting within C_s symmetry produces the global minimum structure XXXIV (C_s, $^1A'$) structure whose geometry is presented in Fig. 1 and the simulated IR-spectrum is shown in Fig. 2. The final XXXIV geometry of Si_3N^- can be considered as a chain $Si_1NSi_2Si_2$ structure. The barrier (XXXIII structure) on the intramolecular rearrangement of the Si_3N^- anion from one XXXIV structure into another is not high (8 kcal/mol at MP2(full)/6-311+G*). The structure XXXV (C_{2v}, $^1A_1$, $1a_1^2 2a_1^2 1b_2^2 3a_1^2$

$1b_1^2 4a_1^2 2b_2^2 5a_1^2 2b_1^2$) is a saddle point with an even lower barrier (7.5 kcal/mol) for the intramolecular rearrangement of the Si_3N^- anion from one XXXIV structure into another.

Our computed adiabatic $EA_a(Si_3N)$ is predicted to be 1.4 eV. The dissociation energies (at QCISD(T) see Table 1) for Si_3N^- into Si^- + Si_2N is 78 kcal/mol.

We also optimized Si_2^+, Si_2, Si_2^-, Si_3^+, Si_3 and Si_3^- (simulated vibrational spectra for Si_3^+, Si_3 and Si_3^- are shown in Fig. 2), because we needed to know the energies of these species at a consistent level of accuracy for the calculations of different dissociation channels of the Si_nN neutral and ionic species. All of these silicon clusters have been previously studied experimentally[27,28] and theoretically,[29] and our results for the silicon dimer and trimer agree well with the previous calculations and available experimental data.

V. MASS SPECTROMETRIC RESULTS

In order to obtain structural information, the Si_3N^+ cations were subjected to a collisional activation (CA) experiment. The resulting fragmentation pattern, obtained upon colliding the 8 keV cluster ions with helium atoms, is shown in Figure 3.

The base peak in the CA spectrum corresponds to the loss of a neutral silicon atom. This Si_2N^+ fragment (m/z 70) contributes to approximately 96 % of the total intensity of the fragmentation processes.[30] In addition to this greatly favored dissociation process, weak signals for the losses of N, SiN and Si_2N are observed (see the 20-fold enlarged region of Figure 3.). The ionic

fragments correspond to Si_3^+ (m/z 84), Si_2^+ (m/z 56) and Si^+ (m/z 28), respectively. Furthermore the collisional activation process leads to a rather small fraction of SiN^+ fragments (m/z 42).

For further insight into the connectivity of the Si_3N^+ cluster ion and to prove the existence of the neutral Si_3N molecule the cation was subjected to a neutralization-reionization experiment, and the resulting NR-spectrum is given in Fig. 4.

The NR-spectrum displays some distinct differences when compared to the results of the CA experiment. The presence of a recovery signal for the reionized Si_3N^+ cations clearly demonstrates that the neutral Si_3N cluster is a viable species in the gas phase. The overall fragmentation pattern is similar to that observed in the CA process. The Si_2N^+ ion contributes strongest to the total ion current. However, a considerably stronger fragmentation of the reionized Si_3N^+ into Si_2^+, SiN^+ and Si^+ can be found. In contrast to the CA mass spectrum (Fig. 3), no signal at m/z 84 that would correspond to the Si_3^+. cation is observed at the detection limit of the machine.

VI. DISCUSSION

According to our calculations, Si_2N, Si_2N^-, and Si_3N form two stable isomers (linear and cyclic) that differ in energy only by few kcal/mol, so both may coexist in the gas phase. The Si_2N^+, Si_3N^+, and Si_3N^- clusters form only one very stable structure, so these species should have a single isomer in the gas phase.

The theoretical results predict the most stable Si_3N^+ cluster to possess a planar rhombic C_{2v} structure (MP2(full)/6-311+G*). In this $^1A_1$ state, the three silicon atoms do not have identical Si-N bond lengths. Rather, two of the

silicon atoms are bonded equivalently (R_e(Si-N)=1.720 Å), and the third silicon atom is coordinated to the nitrogen atom by a considerably longer bond (1.894 Å). The results of the mass spectroscopic experiments can be rationalized by comparing the relative abundance's of the fragment ions with the theoretically derived reaction energies (see Table I). The calculated values predict the fragmentation process of Si_3N^+ into Si_2N^+ and Si to be highly favored energetically. This decomposition pathway is favored over the next lowest lying reaction channel (fragmentation into Si_2N. and Si^+) by 45 kcal/mol (the ΔE values are all taken from the results at QCISD(T) calculations). The process $Si_3N^+ \rightarrow Si_2N^+ + Si$ can be viewed upon as a simple silicon atom evaporation from the cluster molecule Si_3N^+. All other fragmentation channels were calculated to be significantly higher in energy. These results are in excellent agreement with the experimental behavior of this ion as the Si_2N^+ ion accounts for 96 % of the total ion current in the CA process. Nitrogen extrusion from Si_3N^+ to produce the cyclic Si_3^+ (C_{2v} ,$^2B_1$) requires 60 kcal/mol more than the Si_2N^+ + Si formation. The CA spectrum displays only a very weak signal for this process. In the lower mass region of the spectrum, signals for Si_2^+, SiN^+ and Si^+ are observed. The reaction energies for these processes were calculated to lie 92, 143 and 45 kcal/mol higher in energy than the corresponding lowest channel. The "strong" abundance of the Si_2^+ signal relative to Si^+ and SiN^+, can be rationalized by an additional contribution of secondary fragmentation reactions of Si_3^+ and Si_2N^+ that can form Si_2^+ upon collisional activation.

The weak SiN^+ signal agrees well with the energetic predictions as this reaction channel requires 143 kcal/mol more than the Si_2N^+ formation. The extrusion of a nitrogen cation that leads to the formation of the cyclic Si_3 species (C_{2v} $^1A_1$), requires 251 kcal/mol more energy than process 1 and cannot be

detected at all. Thus, the overall fragmentation pattern is in satisfying agreement with the expectation based on the theoretical values.

The Si_2N radical was found to form two different isomers that differ in energy only by a few kcal/mol. The linear SiNSi structure was predicted to be the global minimum, whereas the cyclic structure lies only 4.5 kcal/mol higher.

The NR spectrum gives rise to a relatively small intensity for the survivor ion; this observation points towards quite unfavorable Franck-Condon factors for the charge transfer processes.[30,31] The lowest energy requiring fragmentation of Si_3N is, in analogy to the cationic cluster molecule, silicon atom extrusion accompanied by formation of the Si_2N radical. The reaction energy for the formation of Si_2N and Si was calculated to be only 73 kcal/mol. The next accessible reaction channel ($Si_3N \rightarrow Si_2 + SiN$) requires 53 kcal/mol more than this process. Thus, again in agreement with the experimental results, the reionized Si_2N^+ species represents the major dissociation pathway. In contrast to the fragmentation in the CA process, the NR spectrum does not give rise to Si_3^+ ions. This observation points to the fact that the NR spectrum may be viewed as a superposition of the two mass spectra of Si^+ and Si_2N^+.

VII. CONCLUSIONS

The cationic and neutral Si_3N cluster molecules have been characterized by mass-spectrometric techniques. Their fragmentation behavior in high energy collision experiments corresponds well with the theoretical predictions. High-level ab initio calculations have been used to describe the energetic and structural features of these new molecules. In addition, all experimentally observed ionic and neutral fragment molecules (Si_2N, SiN, Si_3,

Si_2) have been theoretically characterized and their vibrational spectra are reported in order to assist their future infrared spectroscopic characterization.

According to our calculations, the Si_2N, and Si_3N molecules form two isomeric structures that differ by a few kcal/mol which may coexist in the gas phase, while the other clusters (Si_2C, Si_3C, Si_2O and Si_3C) possess one preferred structure.

Upon completion of this work, our colleague, Prof. Michael D. Morse, informed us that he and his co-worker D. J. Brugh have determined[32] that ground electronic state of Si_2N has linear structure with the $^2\Pi_g$ ground electronic state. Their preliminary equilibrium bond length R_e(Si-N) is 1.639 Å is very close to our value R_e(Si-N)=1.631 Å at MP2(full)/6-311+G* and R_e(Si-N)=1.643 Å at QCISD/6-311+G* levels.

ACKNOWLEDGMENT

The work done in Berlin was financially supported by the Deutsche Forschungsgemeinschaft, the Fonds der Chemischen Industrie and the Alexander-von-Humbolt-Stiftung (Max Planck Research Award to H. S.). The work done in Utah was supported in part by the Office of Naval Research and by National Science Foundation Grant #CHE9116286 in Utah.

References and Notes

1 A. Y. Liu and M. L. Cohen, Science 245, 841 (1989); E. Knittle, R. M. Wentzcovitch, R. Jeanloz and M. L. Cohen, M. Nature **337**, 349

(1989);G. M. Nikolic, Vacuum **40**, 143 (1990); W. Schnick, Angew. Chem. Int. Ed. Engl. **32**, 806 (1993); W. Schnick, Angew. Chem. **105**, 1 49 (1993).

2 C. Niu, Y. Z. Lu, and C. M. Lieber, Science 261, 334 (1993)

3 N. N. Greenwood, and A. Earnshaw, *Chemistry of the Elements*, (Pergamon Press, Oxford, 1984).

4 (a) R. R. Lembke, R. F. Ferrante, W. J. Weltner, J. Am. Chem. Soc. **99**, 416 (1977); (c) R. J. VanZee, R. F. Ferrante, and W. Weltner, Jr. J. Chem. Phys. Lett. **139**, 426 (1987); (d) N. Brodie, J.-P. Majoral, and J.-P. Disson, Inorg. Chem. **32**, 4646 (1993); (e) M. Iraqi, N. Goldberg, and H. Schwarz, J. Phys. Chem. **97**, 11371 (1993).

5 (a) R. S. Grev, and H. F. Schaefer, III, H. F. J. Chem. Phys. **80**, 3532 (1984); (b) A. I. Boldyrev, and J. Simons, J. Chem. Phys. **97**, 5875 (1993). (c) A. I. Boldyrev, J. Simons, V. G. Zakrzewski, and W. von Niessen, J. Phys. Chem. in press.

6 For reviews on the physical principles and the scope of the NRMS technique, see: (a) J. K. Terlouw, P. C. Burgers, B. L. van Baar, T. Weiske, and H. Schwarz, Chimia **40**, 357 (1986); (b) C. Wesdemiotis, and F. W. McLafferty, Chem. Rev. **87**, 485 (1987); (c) J. K. Terlouw, and H. Schwarz, Angew. Chem. Int. Ed. Engl. **26**, 805 (1987); d) H. Schwarz, Pure Appl. Chem. **61**, 685 (1989); (e) J. L. Holmes, Mass Spectrom. Rev. **8**, 513 (1989); (f) J. K. Terlouw, Advan. Mass Spectrom. **11**, 984 (1989); (g) F. W. McLafferty, Science **925**, 247 (1990); (h) F. W. McLafferty, Int. J. Mass Spectrom. Ion Processes **118/119**, 221 (1992).

7 For many examples and further references see:(a) N. Goldberg, M. Iraqi, J. Hrusak, and H. Schwarz, Int. J. Mass. Spectrom. Ion Processes **125**, 267 (1993); (b) N. Goldberg, N.; M. Iraqi, J. Hrusak, and H. Schwarz, J.

Phys. Chem. **97**, 10687 (1993); (c) M. Iraqi, and H. Schwarz, Chem. Phys. Lett. **183**, 105 (1993); (d) R. Srinivas, D. K. Bohme, and H. Schwarz, J. Phys. Chem. **97**, 13643 (1993).

8 Common to NRMS and many other mass spectrometry based techniques is that only gross structural features (i.e., atom connectivities) can be inferred from the experiments. Information on geometrical and/or electronic details is, in general, not available. For a review, see: J. L. Holmes, Org. Mass Spectrom. **20**, 169 (1985).

9 (a) R. Srinivas, D. Solzle, T. Weiske, and H. Schwarz, Int. J. Mass Spectrom. Ion Processes **107**, 369 (1990); (b) R. Srinivas, D. Sulzle, W. Koch, C. H. DePuy, and H. Schwarz, J. Am. Chem. Soc. **113**, 5970 (1991); (c) R. Srinivas, D. K. Bohme, D. Solzle, and H. Schwarz, J. Phys. Chem. **95**, 9836 (1991).

10 P. W. Schenk, F. Huber, and M. Schmeisser, in "*Handbuch der Preparativen Anorganischen Chemie*" G. Brauer, Ed.; (Enke Verlag: Stuttgart 1978).

11 H. B. Schlegel, J. Comput. Chem. **3**, 214 (1982).

12 M. J. Frisch, G. W. Trucks, M. Head-Gordon, P. M. W. Gill, M. W. Wong, J. B. Foresman, B. G. Johnson, H. B. Schlegel, M. A. Robb, E. S. Reploge, R. Gomperts, J. L. Anders, K. Raghavachari, J. S. Binkley, C. Gonzales, R. L. Martin, D. J. Fox, D. J. DeFrees, D. J. Defrees, J. Baker, J. J. P. Stewart, and J. A. Pople GAUSSIAN 92, Revision C. (Gaussian Inc., Pittsburgh, P.A.,1992).

13 (a) M. J. Frisch, J. A. Pople and J. S. Binkley. J. Chem. Phys. **80**, 3265 (1984); (b) R. Krishnan, J.S. Binkley, R. Seeger and J.A. Pople. J. Chem.Phys. **72**, 650 (1980); (c) T. Clark, J. Chandrasekhar, G.W. Spitznagel and P.v.R. Schleyer, J. Comput. Chem. **4**, 294 (1983).

14 A. D. Mclean and G. S. Chandler, J. Chem. Phys. **72**, 5639 (1980).

15 R. Krishnan and J. A. Pople, Int. J. Quant. Chem. **14**, 91 (1978)

16 J. A. Pople, M. Head-Gordon and K. Raghavachari, J. Chem. Phys. **87**, 5968 (1987).

17 H. B. Schlegel, J. Chem. Phys. **84**, 4530 (1984).

18 K. P. Huber G. Herzberg. *Molecular Spectra and Molecular Structure.Constants of Diatomic Molecules.* (van Nostrang Reihold Company Publ., N.Y., 1979).

19 (a) S. Saito, Y. Endo and E. Hiroto, J. Chem. Phys. **78**, 6447 (1983). (b) S. C. Foster, K. G. Lubic and T. Amano, J. Chem. Phys. **82**, 709 (1985). (c) C. Yamada and E. Hirota, J. Chem. Phys. **82**, 2547 (1985). (d) C. Yamada and E. Hirota, J. Chem. Phys. **88**, 46 (1988).

20 P. J. Bruna, S. D. Peyerimhoff and R. J. Buenker, J. Chem. Phys. **72**, 5437 (1980).

21 K. A. Peterson and R. C. Woods, J. Chem. Phys. **90**, 7239 (1989).

22 R. Klein, R. P. McGinnis and S. R. Leone, Chem. Phys. Lett. **100**, 475 (1983).

23 (a) W. Weltner, Jr. and D. Mcleod, Jr. J. Chem. Phys. **41**, 235 (1964). (b) Z. H. Kafafi, R. H. Hauge, L. Fredin, and J. L. Margrave, J. Phys. Chem. **87**, 787 (1983). (c) J. D. Presilla-Marquez, W. R. M. Graham, J. Chem. Phys. **96**, 6509 (1992).

24 (a) R. S. Grev, H. F. Schaefer, III, J. Chem. Phys. **82**, 4126 (1985). (b) E. E. Bolton, B. J. DeLeeuw, J. E. Fowler, R. S. Grev, and H. F. Schaefer, III, J. Chem. Phys. **95**, 5609 (1991). (c) C. M. L. Rittby, J. Chem. Phys. 95, 5609 (1991). (d) C. M. L. Rittby, J. Chem. Phys. 96, 6768 (1992).

25 C. M. L. Rittby, J. Chem. Phys. **96**, 6768 (1992).

26 J. D. Presilla-Marquez, and W. R. M. Graham, J. Chem. Phys. **96**, 6509 (1992).

27 (a) L. A. Bloomfield, R. R. Freeman, and W. L. Brown, Phys. Rev. Lett. **54**, 2246 (1985), (b) Q.-L. Zhang, Y. Liu, R. F. Curl, F. K. Tittle, and R. E. Smalley, J. Chem. Phys. **88**, 1670 (1985), (c) W. Begemann, K. H. Meiwes-Broer, and H. O. Lutz, Phys. Rev. Lett. **56**, 2248 (1986), (d) D. J. Trevor, D. M. Cox, K. C. Reichman, R. O. Brikman, and A. Kaldor, J. Phys. Chem. **91**, 2598 (1987), (e) M. R. Nimlos, L. B. Harding, and G. B. Ellison, J. Chem. Phys. 87, 5116 (1987), (f) M. F. Jarrold, and E. C. Honea, J. Phys. Chem. **92**, 5702 (1988), (g) M. F. Jarrold, and E. C. Honea, J. Phys. Chem. **95**, 9181 (1991), (h) T. N. Kitsopoulos, C. J. Chick, A. Weaver, and D. M. Neumark, J. Chem. Phys. 93, 6108 (1990), (i) T. N. Kitsopoulos, C. J. Chick, A. Weaver, and D. M. Neumark, J. Chem. Phys. 95, 1441 (1990), (j) K. Fuke, K. Tsukamoto, F. Misaizu, and M. Sanekata, J. Chem. Phys. **99**, 7807 (1993).

28 M. W. Chase, Jr., C. A. Davies, J. R. Downey, Jr., D. J. Frurip, R. A. McDonald, and A. N. Syverud, J. Phys. Chem. Ref. Data **14**, Suppl. No. 1 (1985)..

29 (a) K. Raghavachari, J. Chem. Phys. **83**, 3520 (1985), (b) K. Raghavachari, J. Chem. Phys. **84**, 5672 (1986), (c) G. Pacchioni, J. Koutecky, J. Chem. Phys. **84**, 3301 (1986), (d) K. Raghavachari, and C. M. Rohlfing, Chem. Phys. Lett. **143**, 428 (1988), (e) K. Raghavachari, and C. M. Rohlfing, J. Chem. Phys. **94**, 3670 (1991), (f) K. Raghavachari, and C. M. Rohlfing, J. Chem. Phys. **96**, 2114 (1992), (g) W. von Niessen, and V. G. Zakrzewski, Ber. Bunsenges. Phys. Chem. **96**, 1228 (1992), (h) W. von Niessen, and V. G. Zakrzewski, J. Chem. Phys. **98**, 1271 (1993).

30 It should be noted that no quantitative measurements were performed that would take into account the varying cross sections for collision and electron-transfer processes of different ions. Also corrections for mass discrimination effects of the ion-detector due to differences in the kinetic energies of the ions were not made.

31 (a) P. Fournier, J. Appell, F. C. Fehsenfeld, and J. Durup, J. Phys. **5B**, L58 (1972). (b) F. C. Fehsenfeld, J. Appell, P. Fournier, and J. Durup, J. Phys. **6B**, L268 (1973). (c) J. C. Lorquet, B. Leyh-Nihaut, F. W. McLafferty, Int. J. Mass Spectrom. Ion Processes, **100**, 465 (1990).

32 D. J. Brugh and M. D. Morse , private communication.

Figure captions

Fig. 1. Computationally optimized geometries at MP2(full)/6-311+G* level of the neutral, cationic and anionic Si_nN and Si_n (N=2,3) species. Geometries at SCF/6-311+G* are given in parentheses. Bond lengths are in Å and bond angles in degrees. Relative energies (in kcal/mol) of Si_3N, $Si_3N^{\pm}$ at theSCF/6-311+G* (in parentheses) and MP2(full)/6-311+G* levels are given under the structuries.

Fig. 2. Simulated calculationally obtained IR-spectra of the neutral, cationic and anionic Si_nN and Si_n (N=2,3) species at MP2(full)/level, except structure III of Si_2N molecule, where calculations were made at QCISD/6-311+G* level (see text).

Fig. 3 Collisional activation (CA) mass spectrum of Si_3N^+ (collision gas helium; 80% transmission (T)).

Fig. 4. Neutralization-reionization (NR) mass spectrum of Si_3N^+ (xenon, 80% T // oxygen 80% T).

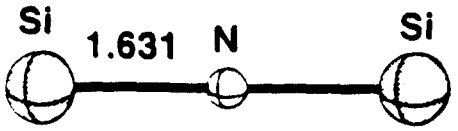

Si_2N^+, I ($D_{\infty h}$, $^1\Sigma^+$)

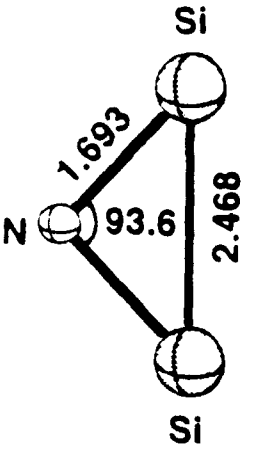

Si_2N, II (C_{2v}, $^2A_1$)

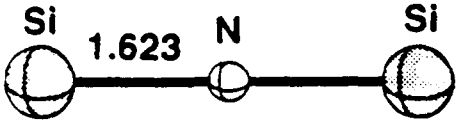

Si_2N, III ($D_{\infty h}$, $^2\Pi_g$)

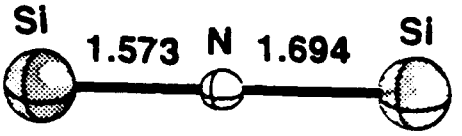

Si_2N, IV ($C_{\infty v}$, $^2\Pi$)

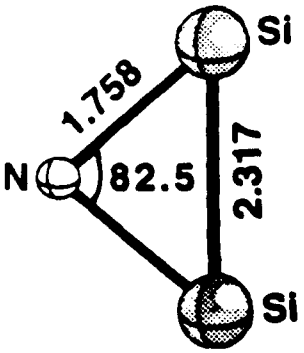

Si_2N^-, V (C_{2v}, $^1A^+$)

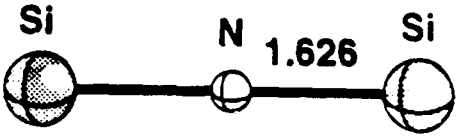

Si_2N^-, VI ($D_{\infty h}$, $^3\Sigma_g^-$)

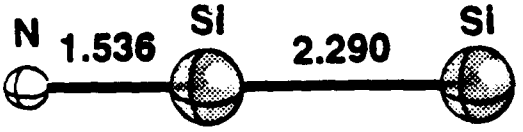

Si_2N^-, VII ($C_{\infty v}$, $^3\Sigma^-$)

Figure 1a.

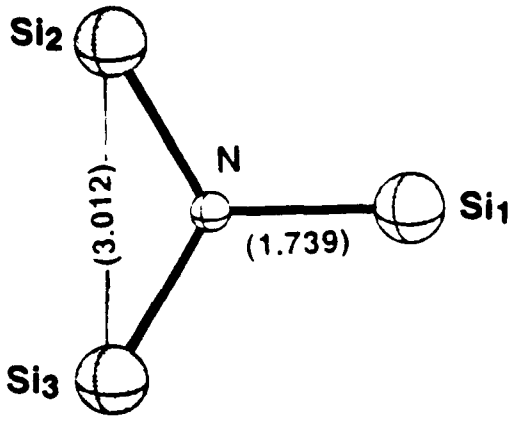

Si_3N^+, VIII (D_{3h}, $^3A_2'$)
(19.1)

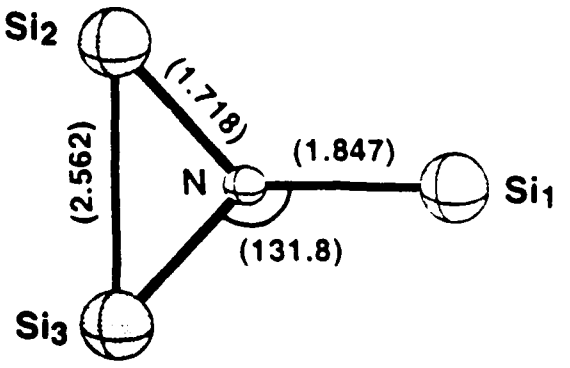

Si_3N^+, IX (C_{2v}, $^3B_2$)
(14.0)

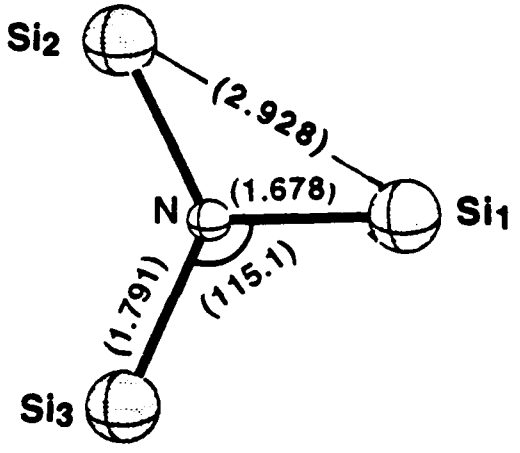

Si_3N^+, X (C_{2v}, $^3B_2$)
(17.3)

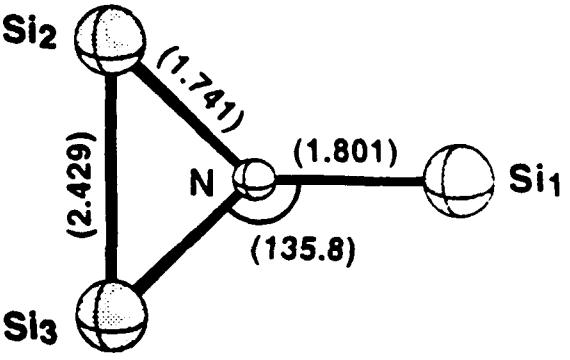

Si_3N^+, XI (C_{2v}, $^3B_1$)
(16.3)

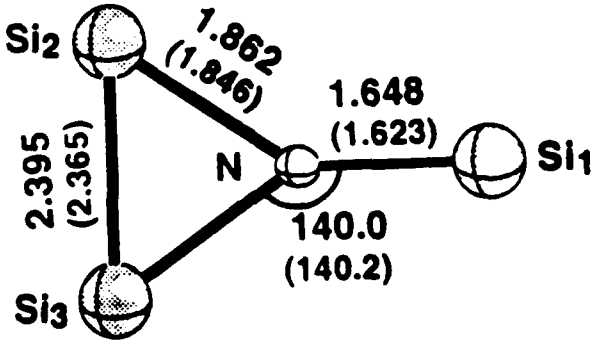

Si_3N^+, XII (C_{2v}, $^1A_1$)
17.9
(7.5)

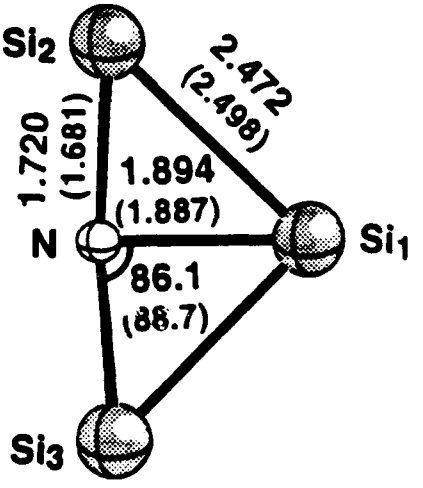

Si_3N^+, XIII (C_{2v}, $^1A_1$)
0.0
(0.0)

Figure 1b.

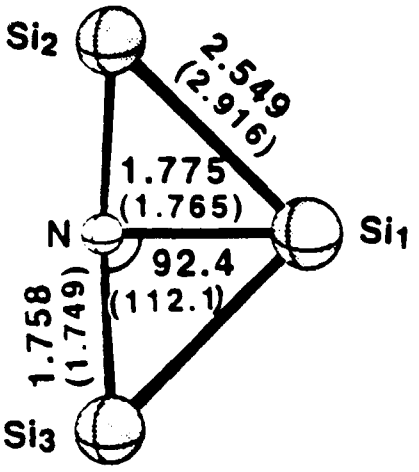

Si_3N, XIV (C_{2v}, $^2A_1$)

9.2
(30.2)

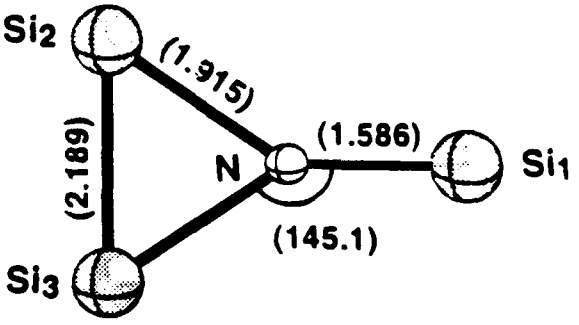

Si_3N, XV (C_{2v}, $^2A_1$)

29.6
(24.2)

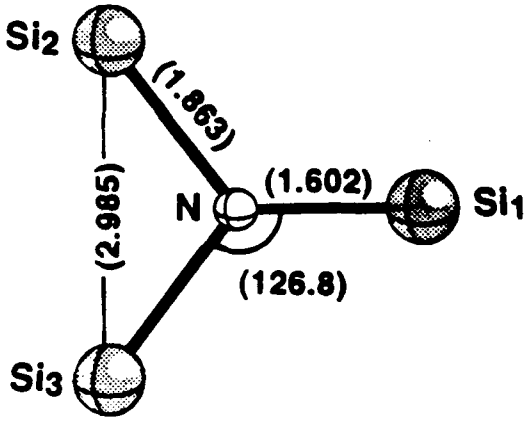

Si_3N, XVI (C_{2v}, $^2A_1$)

102.6
(81.1)

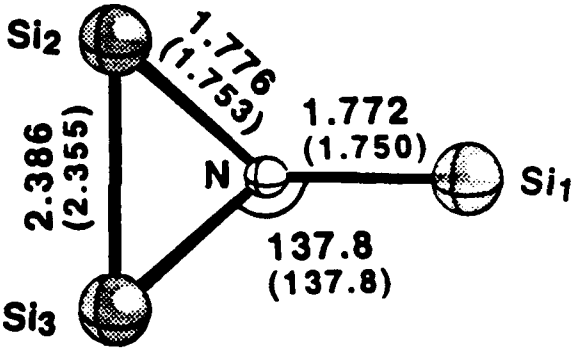

Si_3N, XVII (C_{2v}, $^2B_2$)

3.3
(16.1)

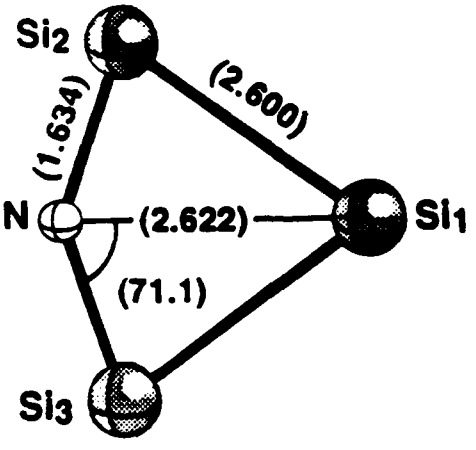

Si_3N, XVIII (C_{2v}, $^2B_2$)

50.5
(58.1)

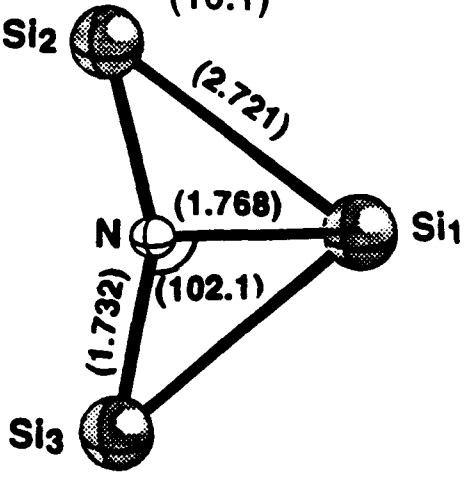

Si_3N, XIX (C_{2v}, $^2B_2$)

59.7
(52.8)

Figure 1c.

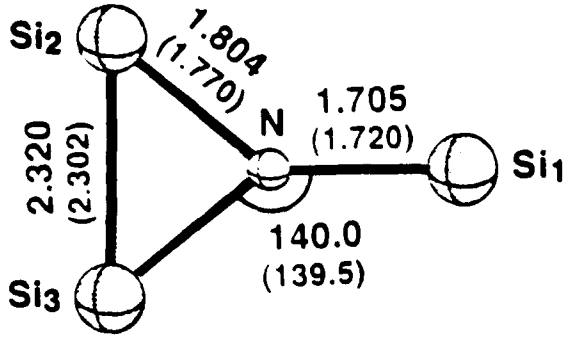

Si_3N, XX (C_{2v}, $^2B_1$)
2.2
(11.2)

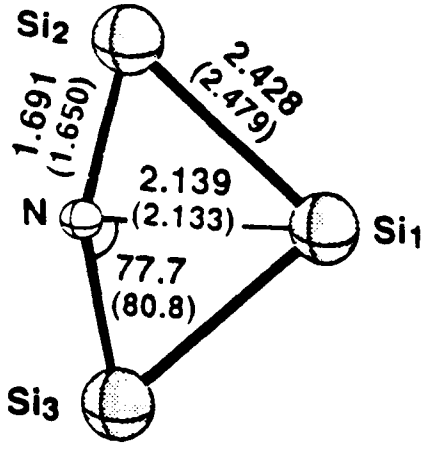

Si_3N, XXI (C_{2v}, $^2B_1$)
0.0
(0.05)

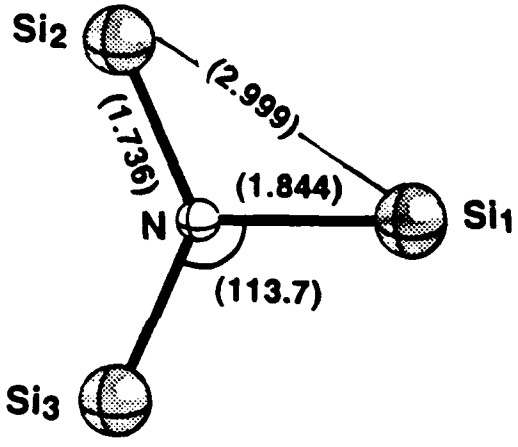

Si_3N, XXII (C_{2v}, $^2B_1$)
81.8
(83.5)

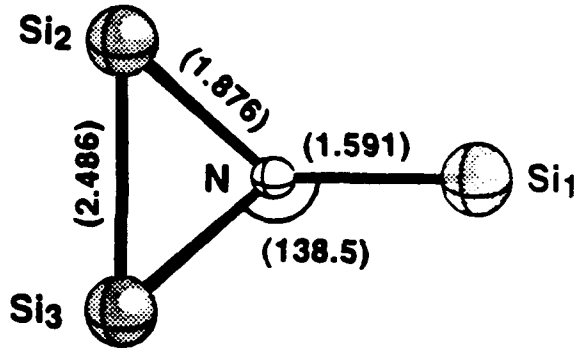

Si_3N, XXIII (C_{2v}, $^2A_2$)
53.9
(52.1)

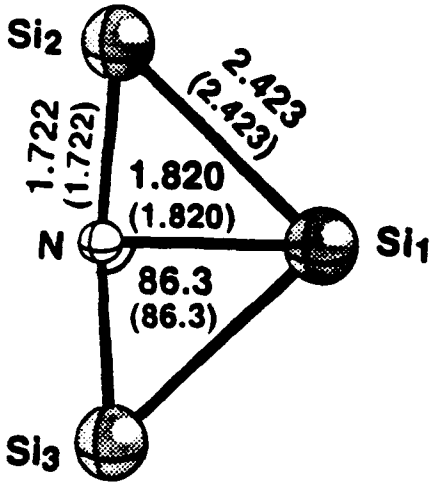

Si_3N, XXIV (C_{2v}, $^2A_2$)
3.8
(0.0)

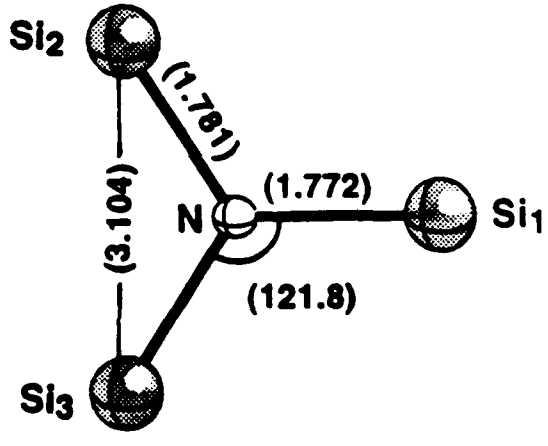

Si_3N, XXV (C_{2v}, $^2A_2$)
46.3
(52.6)

Figure 1d

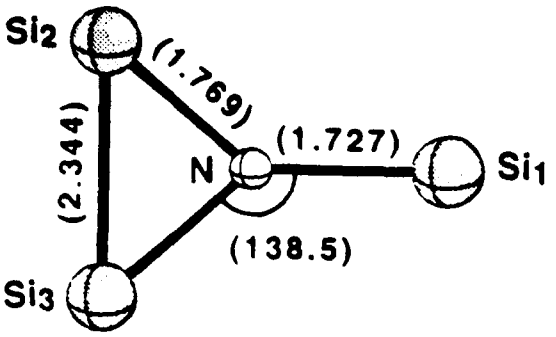

Si_3N, XXVI (C_{2v}, $^4A_2$)

18.5
(36.7)

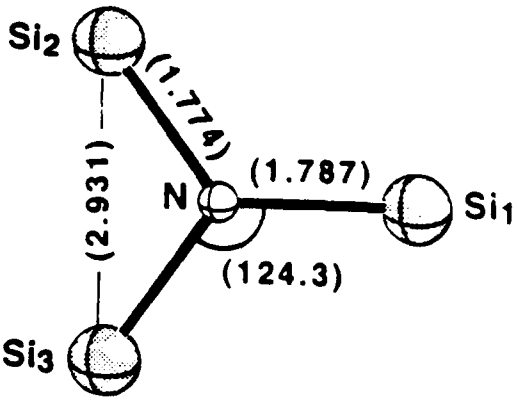

Si_3N, XXVII (C_{2v}, $^4B_1$)

28.3
(47.5)

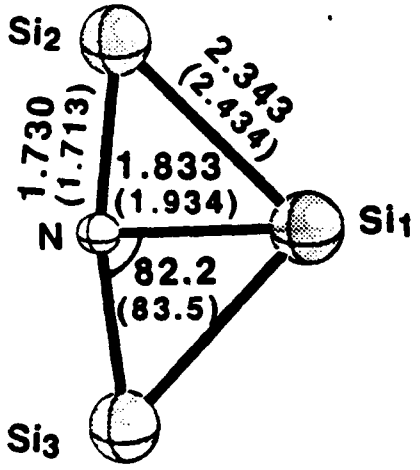

Si_3N, XXVIII (C_{2v}, $^4B_2$)

63.1
(70.7)

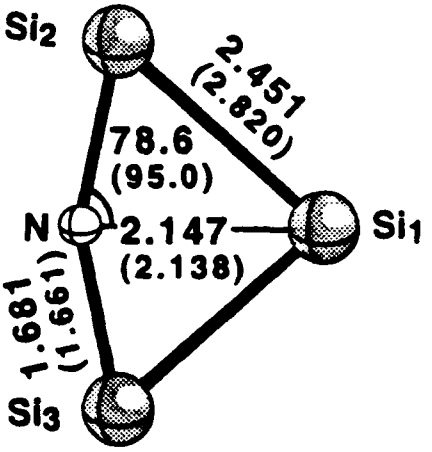

Si_3N, XXIX (C_{2v}, $^4A_1$)

18.6
(35.5)

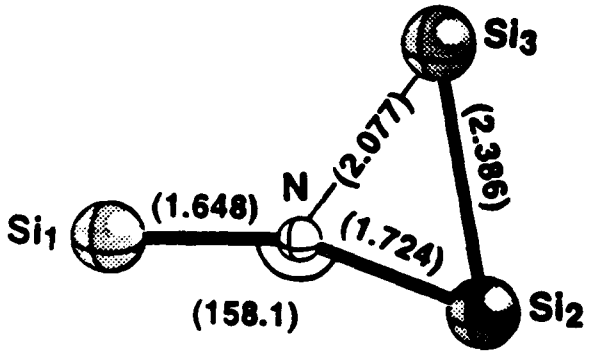

Si_3N, XXX (C_s, $^2A'$)

19.3
(45.6)

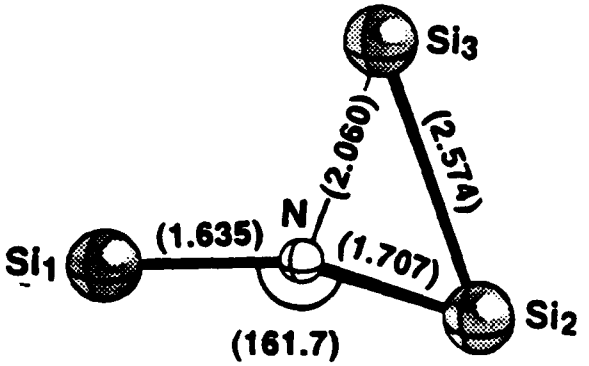

Si_3N, XXXI (C_s, $^4A'$)

18.2
(40.1)

Figure 1e.

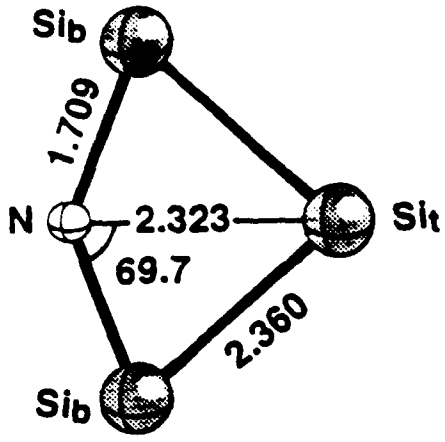

Si_3N^-, XXXII (C_{2v}, $^1A_1$)
18.8

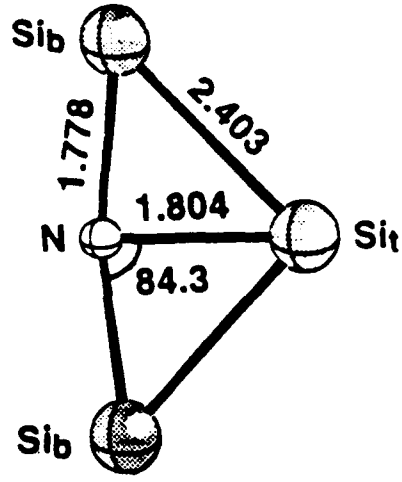

Si_3N^-, XXXIII (C_{2v}, $^1A_1$)
8.1

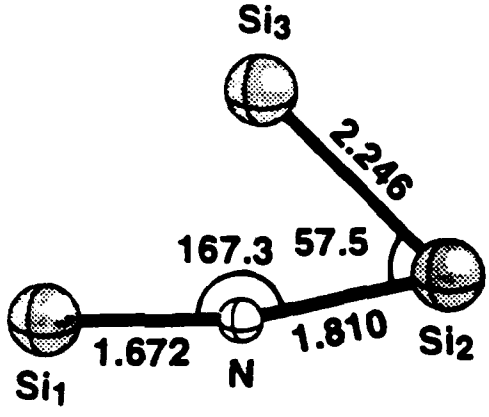

Si_3N^-, XXXIV (C_s, $^1A'$)
0.0

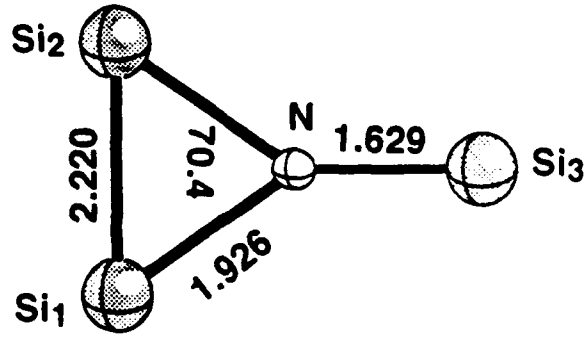

Si_3N^-, XXXV (C_{2v}, $^1A_1$)
7.5

Figure 1f.

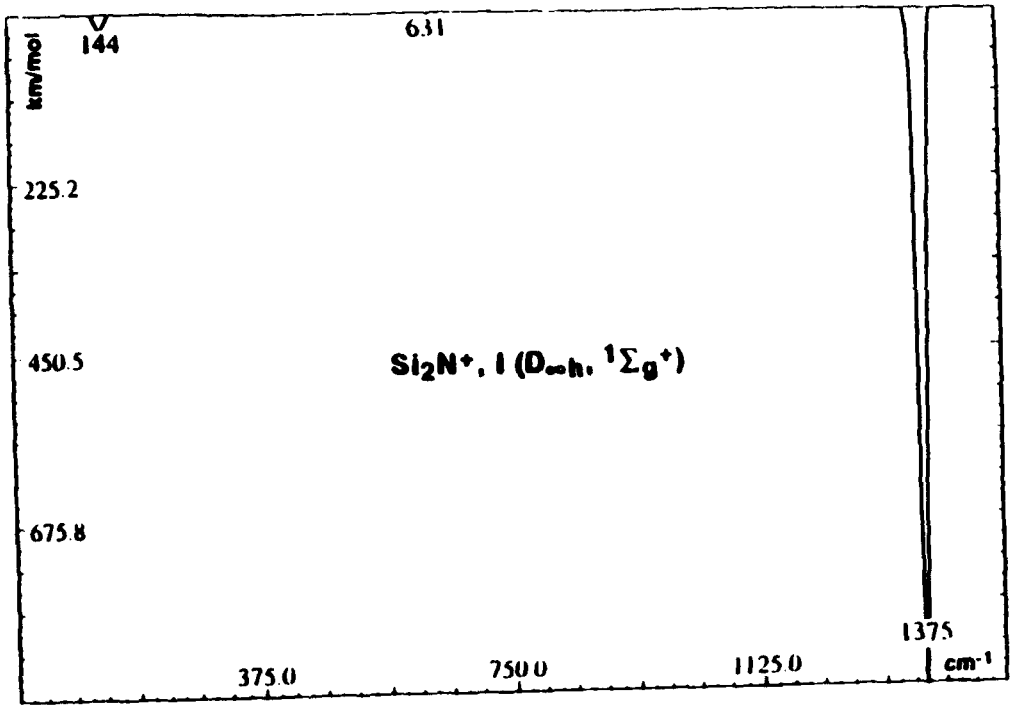
km/mol
144
631
225.2
450.5
675.8
Si_2N^+, I ($D_{\infty h}$, $^1\Sigma_g^+$)
1375
375.0
750.0
1125.0
cm^{-1}

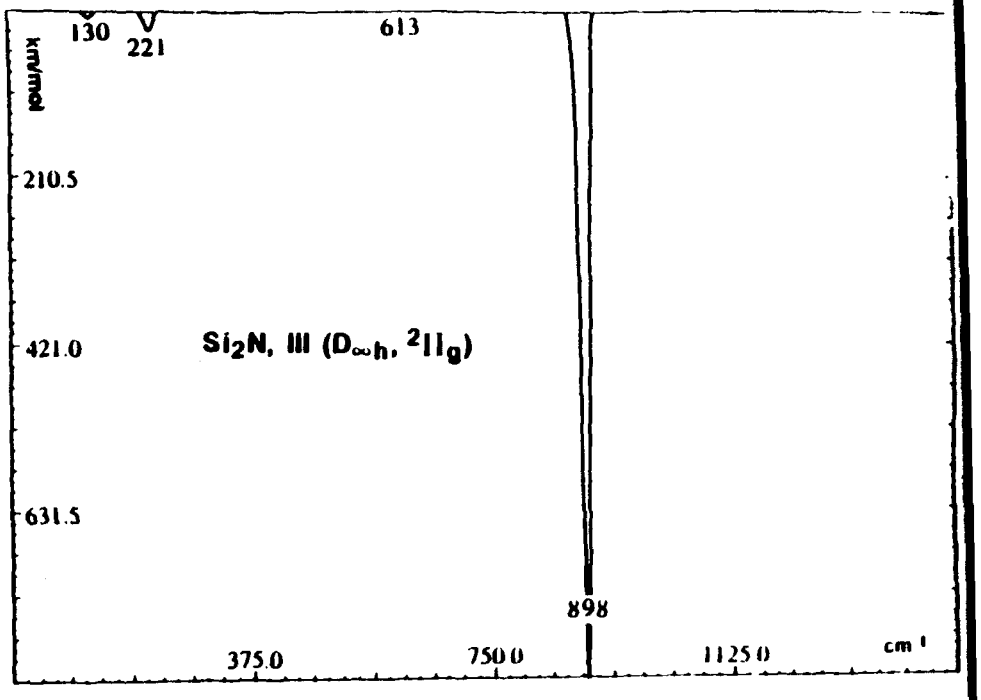
km/mol
130
221
613
210.5
421.0
631.5
Si_2N, III ($D_{\infty h}$, $^2\Pi_g$)
898
375.0
750.0
1125.0
cm^{-1}

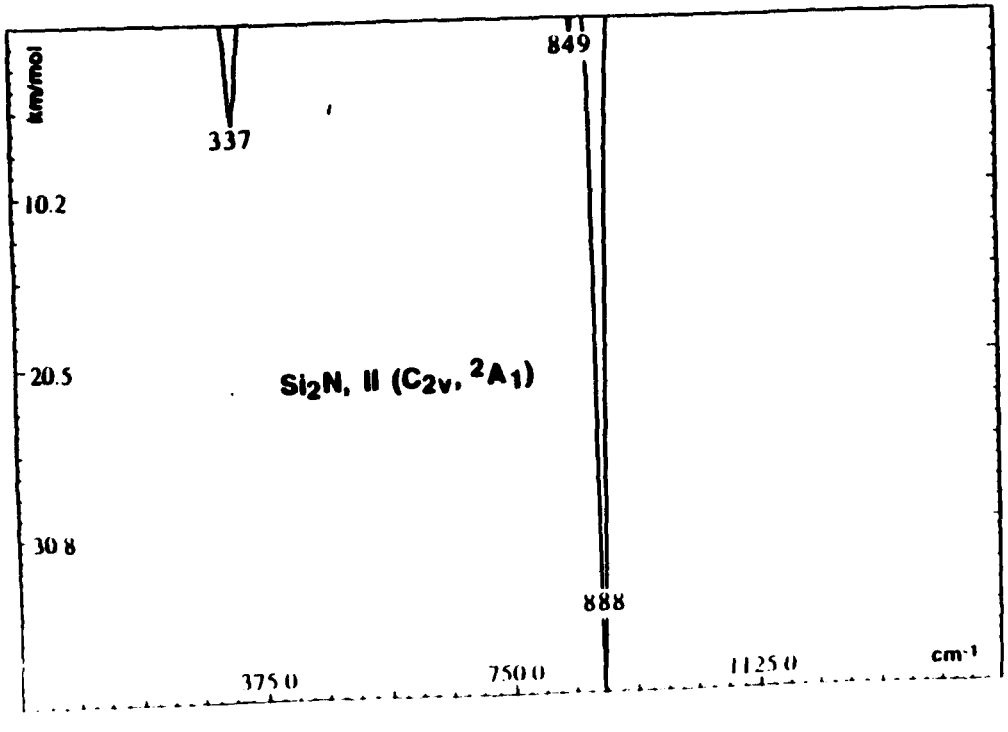
km/mol
337
849
10.2
20.5
30.8
Si_2N, II (C_{2v}, $^2A_1$)
888
375.0
750.0
1125.0
cm^{-1}

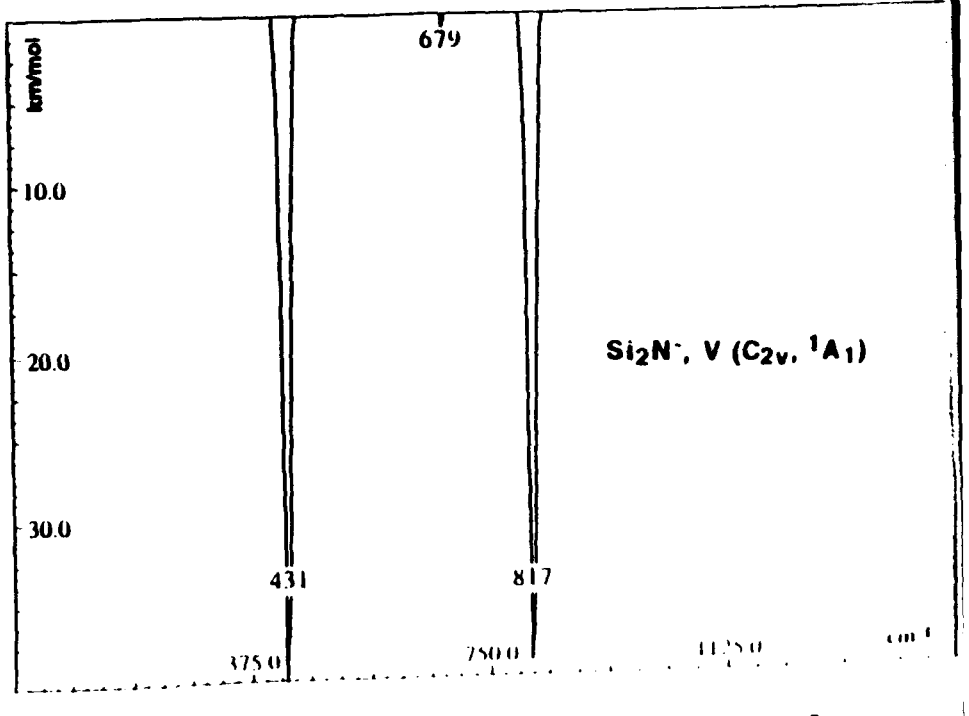
km/mol
679
10.0
20.0
30.0
Si_2N^-, V (C_{2v}, $^1A_1$)
431
817
375.0
750.0
1125.0
cm^{-1}

Figure 2a.

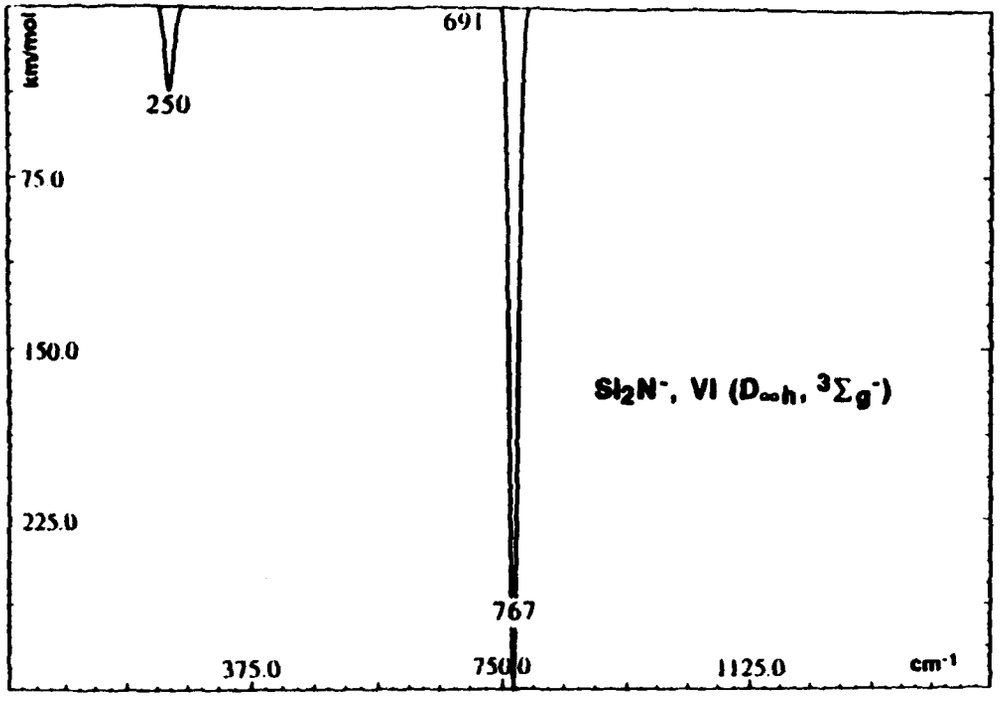
km/mol
250
691
767
75.0
150.0
225.0
375.0
750.0
1125.0
cm-1
Si2N-, VI (D∞h, 3Σg-)

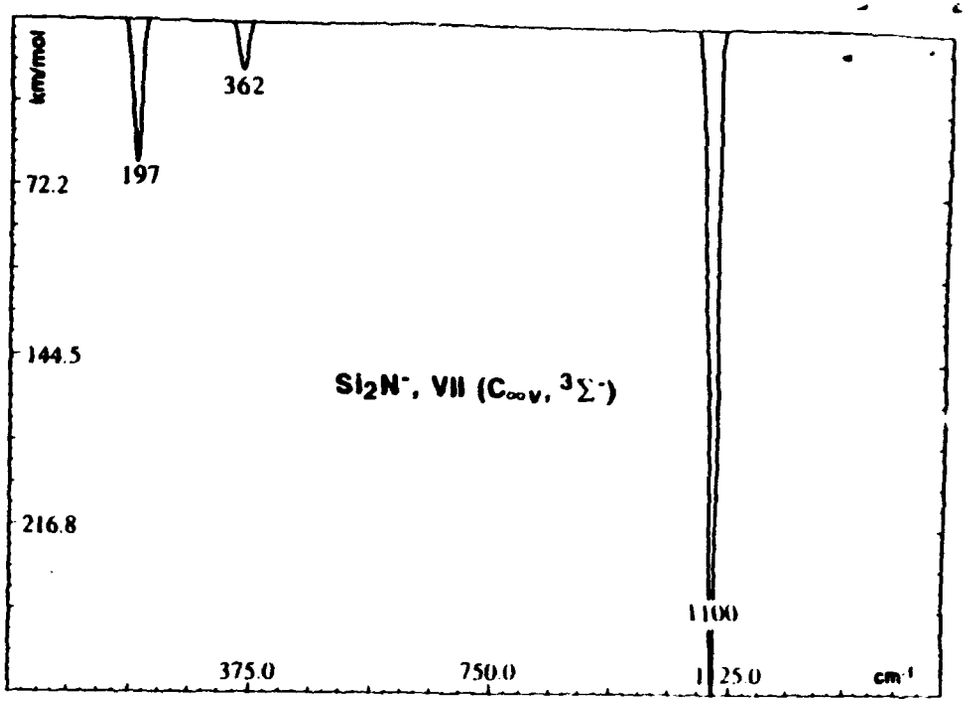
km/mol
197
362
1100
72.2
144.5
216.8
375.0
750.0
1125.0
cm-1
Si2N-, VII (C∞v, 3Σ-)

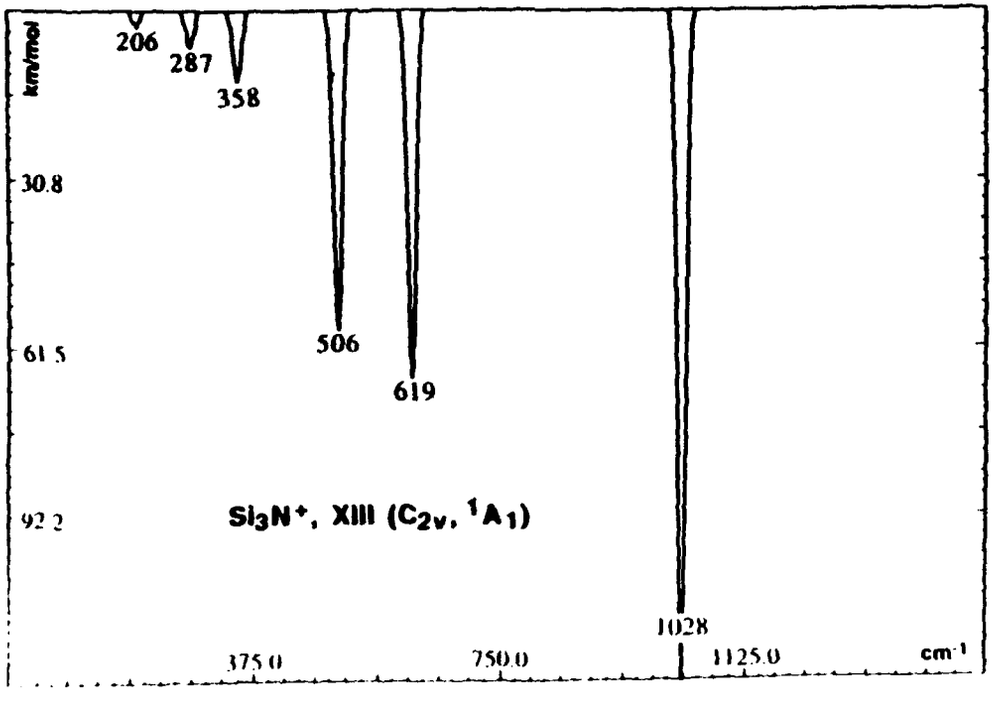
km/mol
206
287
358
506
619
1028
30.8
61.5
92.2
375.0
750.0
1125.0
cm-1
Si3N+, XIII (C2v, 1A1)

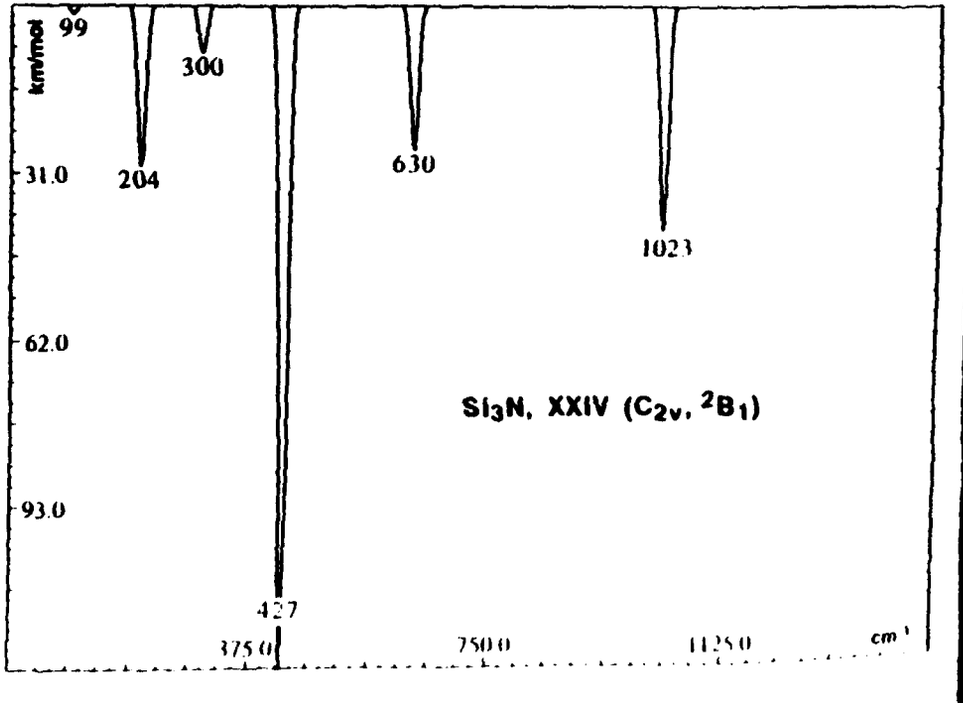
km/mol
99
204
300
427
630
1023
31.0
62.0
93.0
375.0
750.0
1125.0
cm-1
Si3N, XXIV (C2v, 2B1)

Figure 2b.

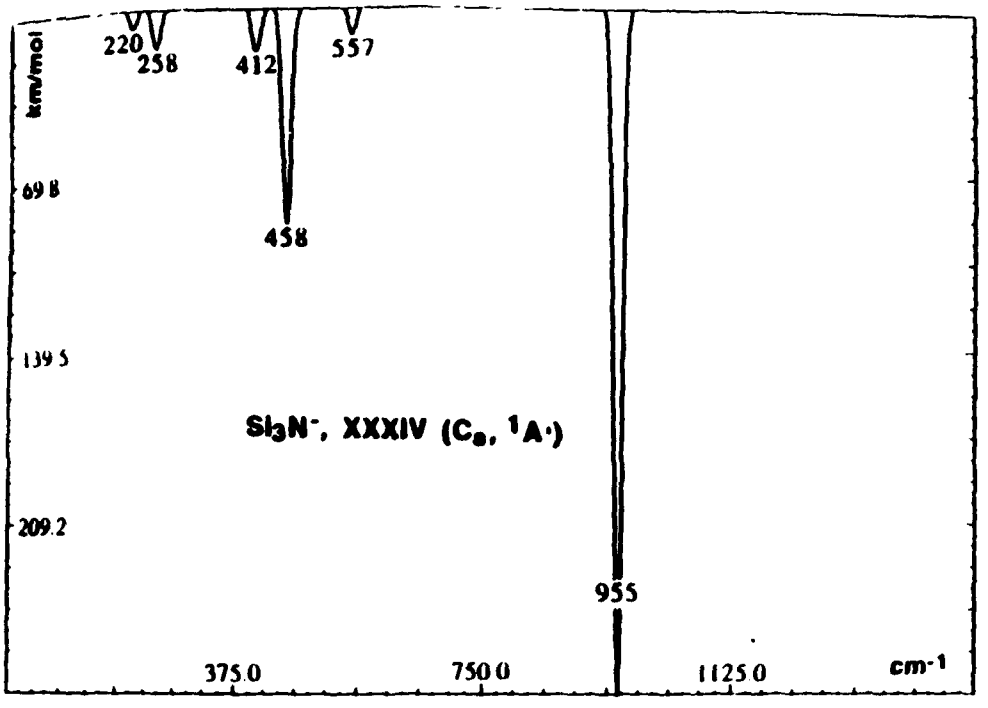
km/mol
69.8
139.5
209.2
220
258
412
458
557
955
Si3N-, XXXIV (Cs, 1A')
375.0
750.0
1125.0
cm-1

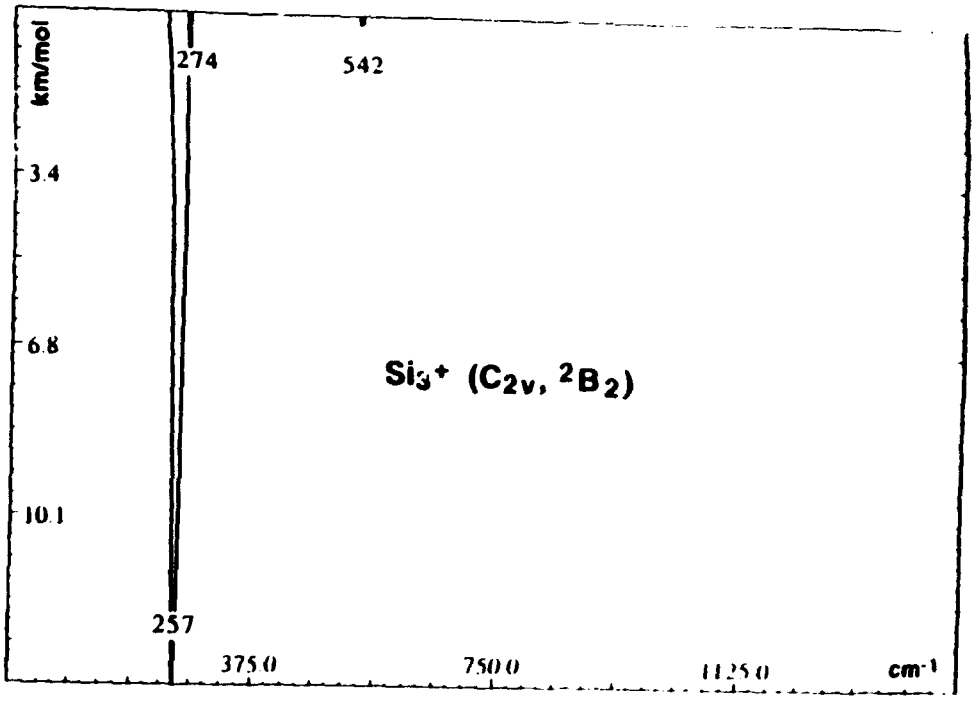
km/mol
3.4
6.8
10.1
274
542
257
Si3+ (C2v, 2B2)
375.0
750.0
1125.0
cm-1

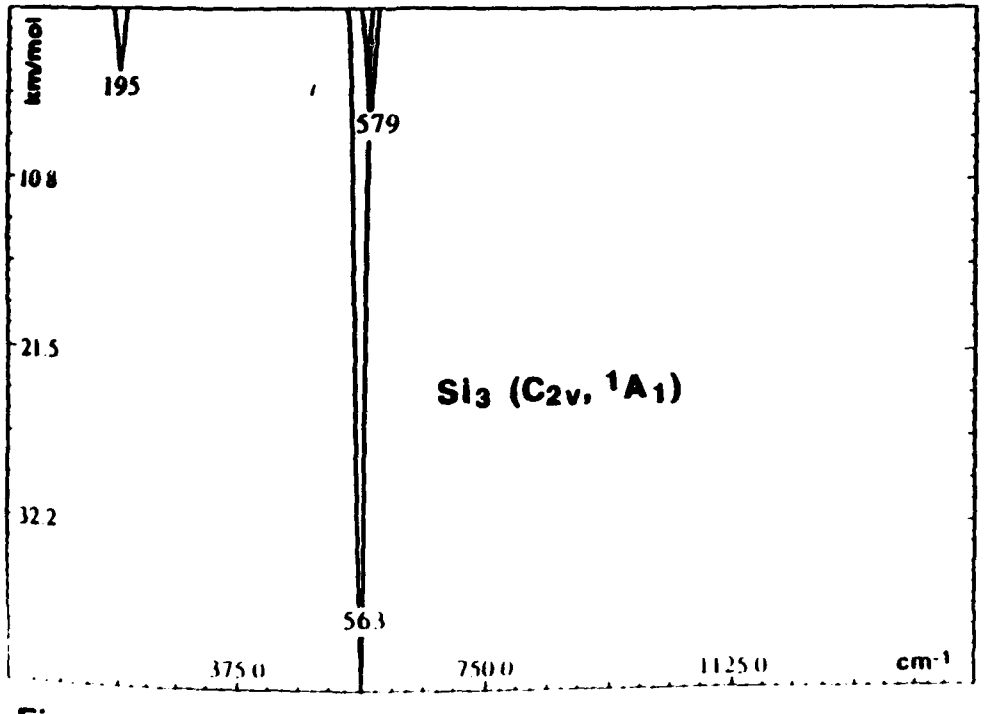
km/mol
10.8
21.5
32.2
195
579
563
Si3 (C2v, 1A1)
375.0
750.0
1125.0
cm-1

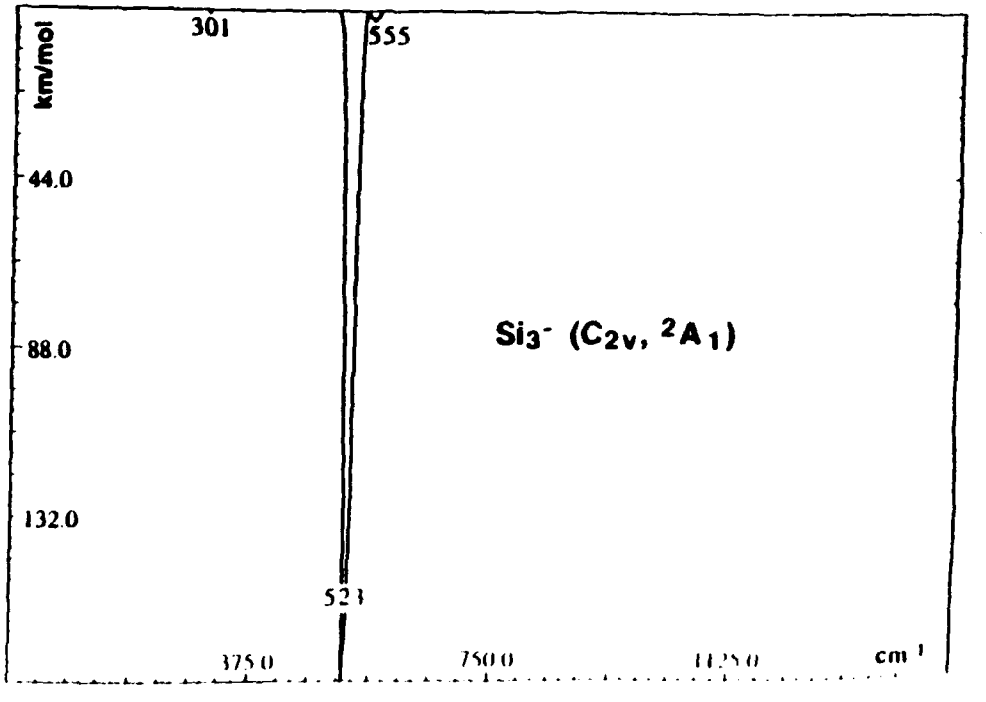
km/mol
44.0
88.0
132.0
301
555
523
Si3- (C2v, 2A1)
375.0
750.0
1125.0
cm-1

Figure 2c.

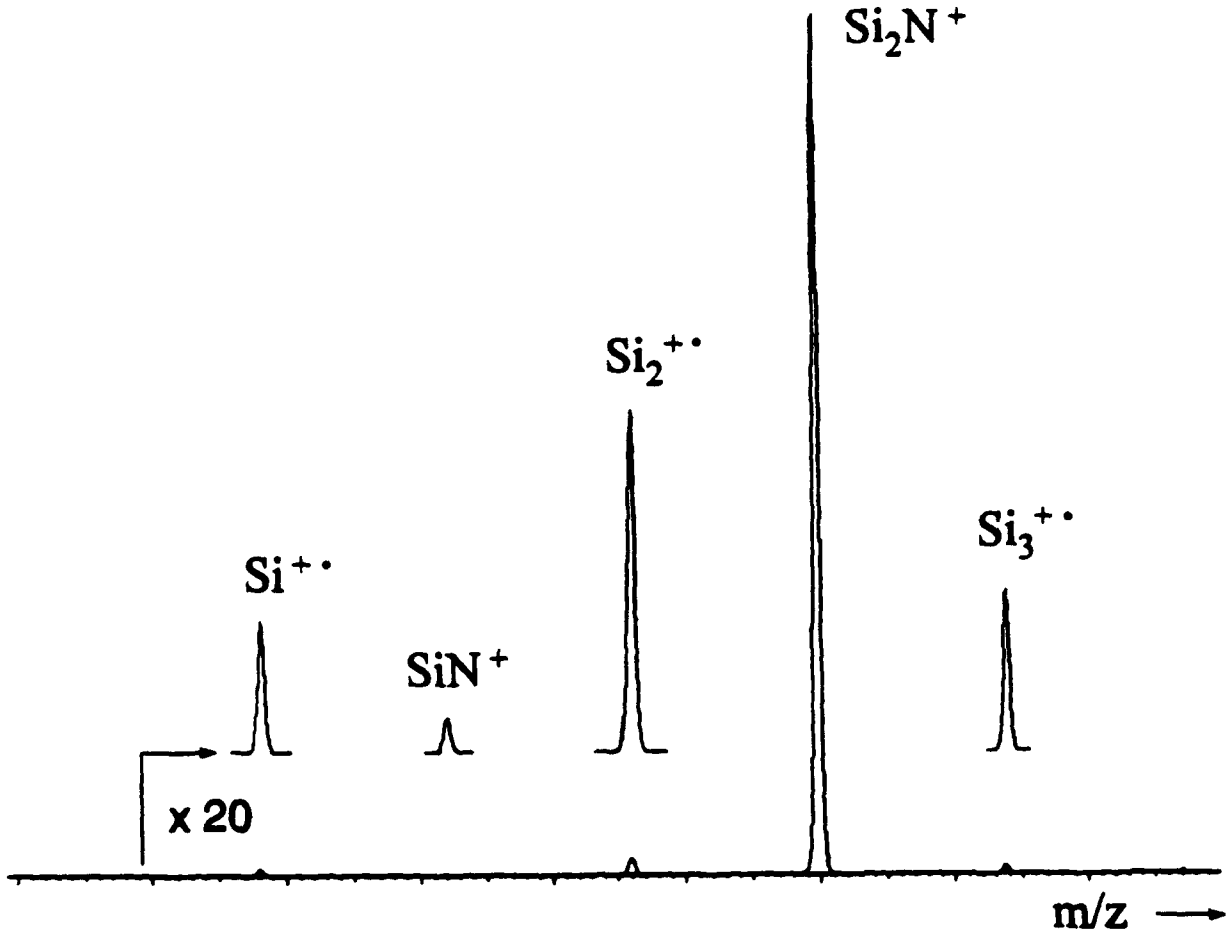

Figure 3.

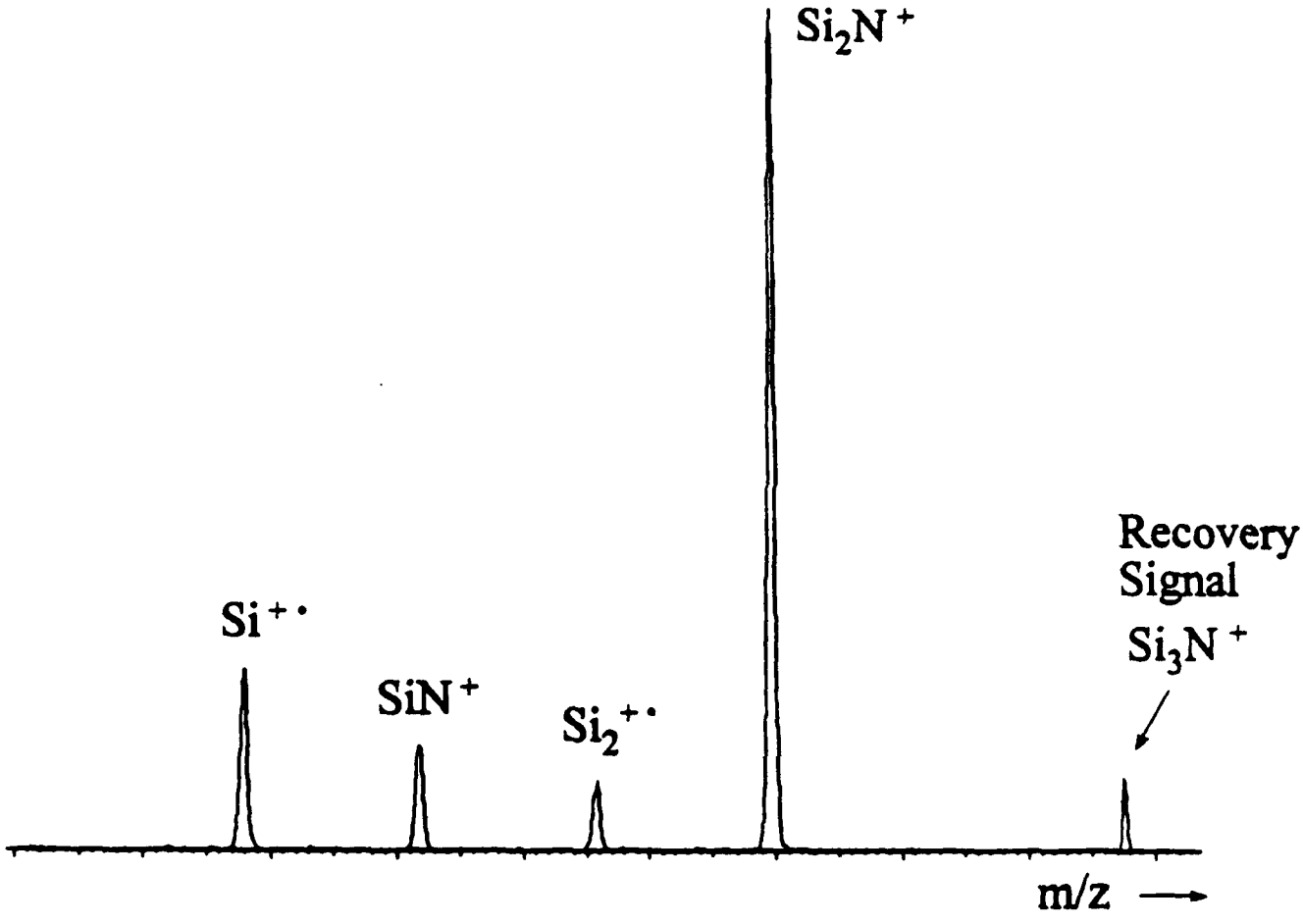

Figure 4.